1. INTRODUCTION:

1.1 Study area background:

This thesis focuses on the structural geological controls of groundwater in a portion of the Limpopo Province of South Africa which falls within the north-eastern section of the Kaapvaal Craton and is underlain almost entirely by Archaean-aged basement lithologies (granite, gneiss and greenstone). More specifically, the study area roughly forms a 100km x 200km rectangle which is bordered to the south by the Thabazimbi-Murchison Lineament (TML). In the east, basement lithologies are bounded by the Drakensberg Group volcanic rocks (Karoo Supergroup) of the Lebombo Mountains associated with the eastern margin of the Kaapvaal craton. The northern margin is bound by the Palala Shear Zone and Central Zone of the Limpopo Belt and the western margin is delineated by intrusive rocks of the northern lobe (Potgietersrus Limb) of the Bushveld Igneous Complex (refer to Figure 1).

The north-eastern section of the Kaapvaal Craton mainly consists of Palaeo-, Meso- and Neoarchaean intrusions with later supracrustal rocks covering some of the edges of the study area. Due to its old age, this part of the continent has existed long enough to experience numerous geological events which, when combined, results in a complex structural character of the geology in the area. Semi-arid regions of the Limpopo Water Management Area (WMA1) characterize the eastern section of the study area; whereas subtropical conditions with higher rainfall are found west of the northern escarpment in the Levuvu/Letaba Water Management Area (WMA2) (refer to Figure 2).

According to the national census of 2001, the Limpopo Province is home to about 11.8% of South Africa's total population (refer to Figure 3). The national census of 1996 states that 89% of Limpopo's inhabitants live in non-urban areas and many of those people make a living through subsistence farming. Apart from subsistence farming, a large part of the Limpopo Province's income comes from agriculture. Citrus, tomatoes, table grapes, sunflowers, maize, cotton, peanuts, bananas, litchis, pineapples, mangoes, paw paws, tea and coffee are grown on a commercial basis (GCIS 2004). Furthermore, cattle farming, game ranching and game hunting also contribute to the commercial agricultural activities of the province (GCIS 2004). Evidently a lot of water is necessary to run all of the agricultural activities in the area. 78% of the households in the Limpopo Province have piped water, but often only from a communal tap (SSA 2003). The need for irrigation and household water has placed a greater demand on groundwater resources and further groundwater exploration is required in this area.

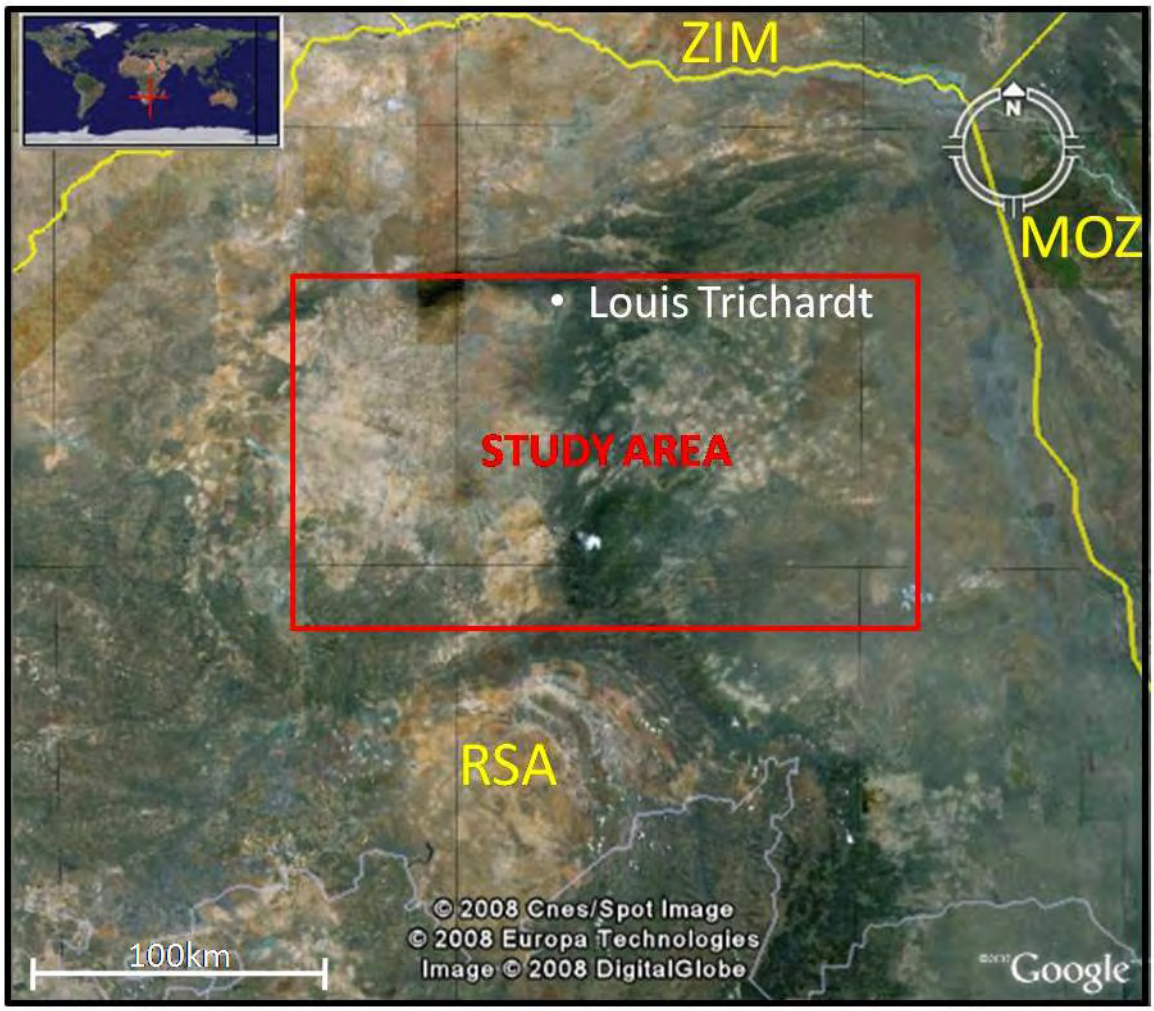

Figure 1: A Google Earth© image indicating the location of this project's study area.

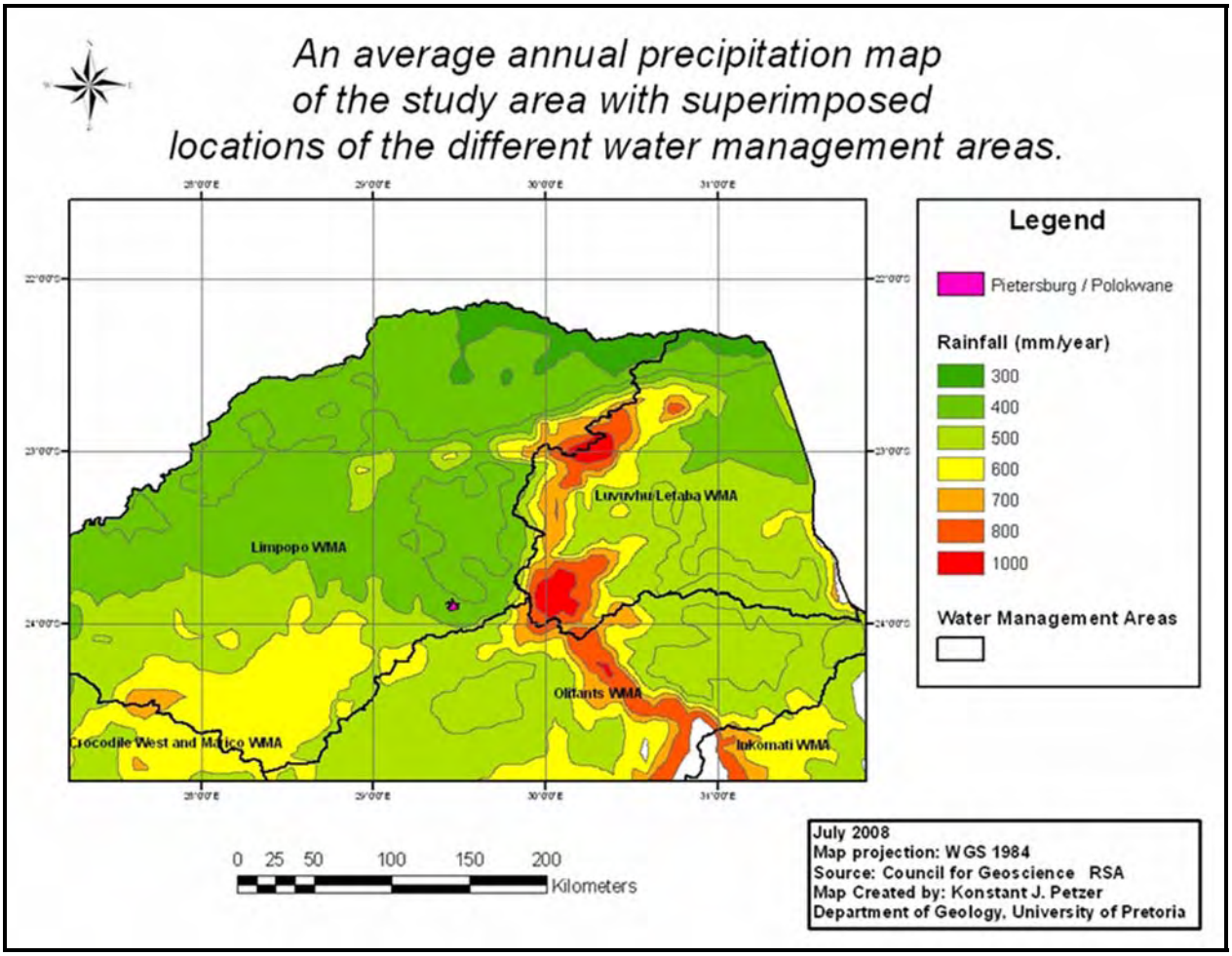

Figure 2: An average annual precipitation map of the study area, which falls within the Limpopo- (WMA1) and Levuvu/Letaba- (WMA2) water management areas.

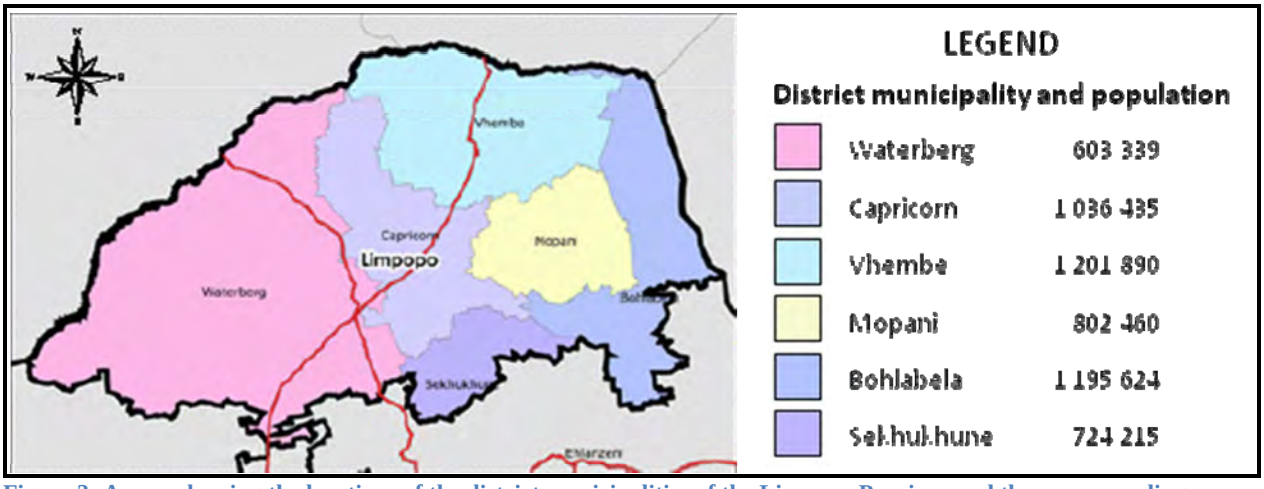

Figure 3: A map showing the locations of the district municipalities of the Limpopo Province and the corresponding population of each. Source: The South African Demarcation Board and Statistics South Africa, 2000.

1.2 Problem statement:

An investigation into the correlation between structural geology and the flow/occurrence of groundwater in the basement lithologies of the Limpopo Province in South Africa.

1.3 Objectives:

Primarily, this investigation aims to examine the structural geology of the Limpopo basement lithologies. Once the structural interpretations have been made, the investigated structures will be compared to the groundwater data in order to determine whether or not there exists a spatial correlation between the structural elements and the flow or presence of groundwater in different parts of the basement aquifers. Since drilling for groundwater is an expensive practice, the knowledge gained through this study and the possible correlation between groundwater flow/occurrence compared to structural geology, might improve the odds of finding groundwater and save a lot of money. Moreover, the discovery of groundwater could improve the living conditions of some of the inhabitants of the Limpopo Province and help to boost the province's economic growth through enhanced productivity of commercial agriculture.

1.4 Scope and limitations of the study:

Although the study area is extremely large (~ 20 000km^2), the extent of outcrops are remarkably limited in some of the regions due to weathering and soil cover. This makes it difficult to trace structures from one area to the next with a lack of intervening outcrop. The sheer size of the study area limits the amount of detail with which the total area could be mapped. Due to the long geological history and relatively small amount of outcrops, it is difficult to accurately recreate an exact geochronological timeline of the numerous events that took place by using relative age relationships only. Therefore, the focus of this study is more on understanding the orientation of structures presently in the rocks (as this is what influences the flow of groundwater) than it is on interpreting a detailed tectonic history. Nevertheless, where possible, geochronology was taken into consideration and related to isotopic and relative ages described in literature. However, literature on the structural geology of the basement lithologies is very limited. Lastly, the author had to rely heavily on interpolated data between existing boreholes instead of drilling precisely on structures recognized in the field.

1.5 Methodology:

Relevant literature was collected and studied in order to have a thorough understanding of the field area. As the study progressed and new ideas came to mind, more sources of literature were consulted. The information gathered from this stage of the project was compiled into the literature review found below (Chapter 2).

As in most exploration projects, remote sensing was used during the early stages of this project. Aerial photographs of one area in WMA1 and a N-S line through WMA2 were studied stereoscopically in order to gain a three-dimensional view of the topography and the regional structures in the area. Observed structures were then compared to structures described in the literature study and marked as targets for field investigation. For a more regional survey, satellite images from Google Earth were also viewed for a preliminary regional structural interpretation. Aeromagnetic data from the study area was also acquired from the Council for Geoscience of South Africa, which mainly indicated the presence of dolerite dykes and major faults.

A number of field excursions were undertaken to cover the study area as thoroughly as possible with available time, finances and access to property all playing a constraining role. Large areas without measurable outcrops, as well as areas with structureless outcrops (usually post tectonic) were also unfortunately encountered. At each location with measurable structures, a waypoint was marked with a GPS. A compass-clinometer was then used to measure dips and strikes of planes (mostly joint planes, but also fault planes, foliation planes, fold axial planes, bedding planes and contacts). Trends and plunges of lineations such as the traces of veins, hinge lines, sense of fault/shear movements (including slickenside lineations), traces of dykes and the trend of rivers were also measured using the compass. All the measurements were initially recorded in a field notebook and were later transferred to a computer database. Sketches were drawn in the field notebook of some of the more interesting/involved structures to help solve the complex nature of the structural geology. Many scaled photographs were also taken of the structures found in the field to serve as visual aids during data interpretation. The emplacement sequences and relative age relationships of rocks and structures were recorded where possible, but as mentioned before, geochronology was not the main focus of this study.

The computer database was then analyzed further. Structural measurements from the database were stereographically projected, using Spheristat 2.2 software. Poles to planes were plotted and density distributions of these poles were also created in order to find

preferred orientations of structures. Coordinates from the GPS were plotted onto an ArcGIS geology base map of the study area. The orientations of the structures were then related to their GIS coordinates in order to identify the spatial relationships of the structures and to identify possible dominant orientations. Since brittle structures (such as joints) with different three-dimensional orientations don't all form under the same stress-strain conditions, such structures were subdivided into groups. Each group of structures was then analyzed based on its orientation, distribution and possible relationship to the lithologies in which it occurs.

A database containing groundwater data of most of the boreholes in the area was obtained from (Groundwater Resources Information Project "GRIP"). Each of the boreholes was also plotted on the GIS map. Special attention was paid to the transmissivity and yield values from each borehole. In simple terms, transmissivity is defined as the ability of an aquifer to transmit water. More specifically, transimissivity is the rate at which water of the prevailing kinematic viscosity is transmitted through a unit width (i.e. 1 meter) of an aquifer under a unit *hydraulic gradient.* Transmissivity is equal to an integration of the hydraulic conductivities across the saturated part of an aquifer, perpendicular to the flow paths and is measured in cubic meters per day (Horton, 1999).

$$T = Kb$$

Where T = Transmissivity, K = Hydraulic Conductivity and b = the saturated thickness of the aquifer.

Yield is defined as the quantity of water from a groundwater source, expressed as a rate of flow (m^3/s) in this case, that can be collected for a given use (adapted from Willmitzer, 2008). Transmissivity- and yield values of the boreholes were spatially interpolated through inverse distance weighting (see appendix for explanation) to see if any spatial patterns or trends could be identified. Although the interpolated maps still appear quite random, better correlation between inverse distance weighted interpolations and geological features were observed than when other geostatistical methods such as kriging were used. The spatial trends in water occurrence and flow were then related to the lithologies and geological structures at the boreholes' locations to determine whether or not any correlations exist.

2. LITERATURE REVIEW:

2.1. Regional Geology:

2.1.1. General:

Although Archaean crystalline basement rocks characterize the study area, other lithologies which outcrop locally and in adjacent areas will also be considered in this thesis, as many of the post-Archaean geological structures are not limited to the basement rocks alone, and often cross-cut younger strata preserved nonconformably above the basement rocks. Since the supracrustals have undergone less weathering and erosion than their basement predecessors, tectonic events that occurred during or after supracrustal formation are often better preserved in these younger rocks.

Unfortunately the extremely large area covered by the basement rocks alone influenced the author to only include previous supracrustal data found in existing literature. One of the main aims of this study is to identify structures in the basement rocks that could influence the occurrence and movement of groundwater. Below is a geological map of the area and a timeline of emplacement events to familiarise the reader with the area.

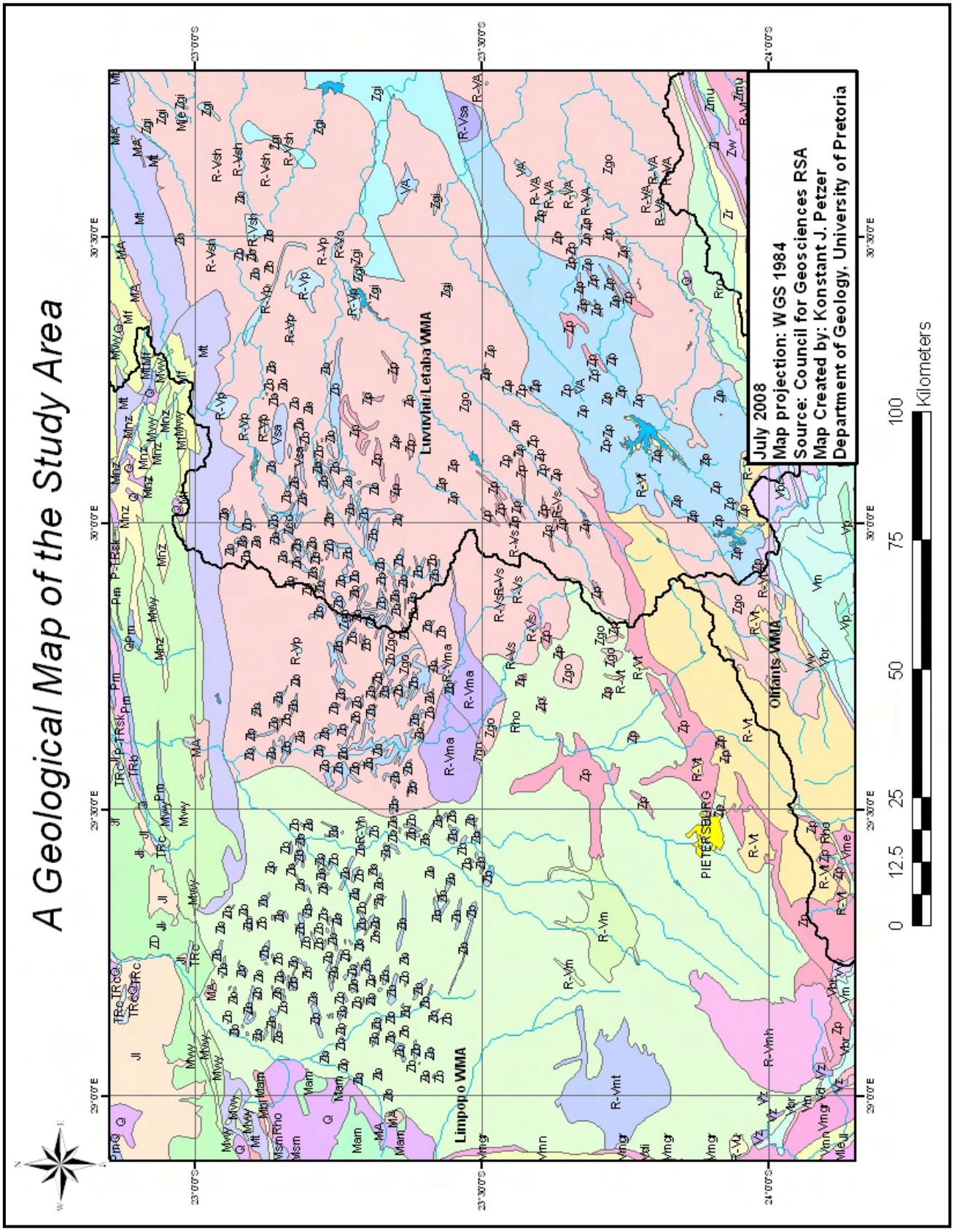

Figure 4: A Geological Map of the Study Area. Refer to legend on next page.

Stratigraphic Units and Legend for Geology Map

Table 1: Geological timeline of igneous/metamorphic lithological emplacements/events (Modified after Robb et al., 2006)

Unit/locality	Sample nature	Age in Ma. (method if available)	Ref.
Goudplaats-Hout River Gneiss	Migmatitic tonalite gneiss	3333 ± 5 (C)	1
Goudplaats-Hout River Gneiss	Tonalite gneiss	3282.6 ± 0.4 (C)	2
Goudplaats-Hout River Gneiss	Tonalite gneiss	3274 +56/-45 (A)	2
Makhutswi Gneiss	Trondhjemite and Tonalite gneiss	3228 ± 12 (A)	3
Giyani Greenstone Belt	?	3202.3 ± 2 (?)	10
Central KV Craton stable	----------	3100	10
Harmony Granite	Trondhjemite gneiss	3091 ± 5 (A)	4
Murchison Greenstone Belt	----------	3090 - 2970	3, 11
Makhutswi Gneiss	Tonalite gneiss	3063 ± 12 (A)	4
Baderoukwe Gneiss	Trondhjemite gneiss	3018 ± 15 (A)	5
Discovery Granite	Granite	2969 ± (A)	5
Gneisses in the Matlala and Moletsi vicinity	Migmatitic and non-migmatitic biotite gneisses	2940-2870 (C)	Unp ubl.
Melkboomfontein Granite	Granite	2853 +19/-18 (A)	2
Gravelotte area	Pegmatite	2848 ± 58 (A)	4
Willie Granite	Porphyritic granite	2820 ±38 (A)	5
Cunning Moor Tonalite	Massive, homogenous tonalite	2784 ± 53 (Rb-Sr whole rock)	12
Turfloop Granite	Porphyritic granodiorite	2777 ± 10 (A)	6
Turfloop Granite	Monzogranite	2765 ± (A)	2
Turfloop Granite	Porthyritic granodiorite	2763 ± 15 (A(T))	6
Rooiwater Complex	Hornblende tonalite	2740 ± 4 (A)	3
Dolerite dykes (Ventersdorp related)	Dolerite	2.7 Ga.	13
Limpopo orogeny	Bulai Gneiss	2.57 – 2.66 Ga. Minimum age	14
Mashishimale Suite	Peraluminous granite	2698 ±21(A)	5
Lekkersmaak Granite	Porphyritic granite	2690 ± 65 (A)	7
Uitloop Granite	Granite	2687 ± 2 (A)	8
Matok Granite	Charno-enderbite	2671 ± (C(?))	9
Palmietfontein Granite	Granite	2456 ± 78 (Rb-Sr whole rock)	13
Reactivation of Palala	------	2.0 Ga.	15

Unit/locality	Sample nature	Age in Ma. (method if available)	Ref.
Bushveld Igneous Complex	-------	2.06 Ga.	
Blouberg Fm.	Alluvial sandstones	2.0 – 1.9 Ga.	
Waterberg Gp.	Sedimentary	>1.85 Ga.	
Soutpansberg Gp.	sst	1.85 Ga.	
Extrusion of Drakenberg Flood Basalts	Basalt	180 Ma.	

Methods: **A = U-Pb ID-TIMS; C = Pb-Pb zircon evaporation; (T) = Titanite. Mineral analyse zircon, unless otherwise mentioned.**
References: **1. Brandl and Kröner (1993); 2. Kröner et al. (2000); 3 Poujol et al. (1996); 4. Poujol and Robb (1999); 5 Poujol (2001); 6. Henderson et al. (2000); 7. Walraven (1989); 8. De Wit et al (1993); 9. Barton et al. (1992); 10. Kröner et al. (2000); 11. Brandl et al. (1996); 12. Robb et al. (2006), 13. Uken & Watkeys (1997); 14. McCourt & Armstrong, (1998); 15. Bumby et al. (2004).**

2.1.2. Kaapvaal Craton:

The Kaapvaal Craton formed and stabilized between 3.7 - 2.7 Ga. and covers about 1.2 $x10^6$ km^2 (de Wit et al., 1992). Growth of the craton during this time was achieved by processes of initial separation of continental lithosphere from the mantle, followed by tectonic accretion of crustal fragments to form the various granite-greenstone subdomains (de Wit et al., 1992). The oldest Kaapvaal rocks are preserved in the Barberton area, in the eastern domain of the craton. Growth of the Kaapvaal Craton likely took place by accretion onto its northern edge, as recorded by a series of ENE-trending subdomains, and on the western edge of the craton (NNW-trending subdomains).

The northern domain (ca. 3.25 – 2.7 Ga.) of the Kaapvaal Craton (the focus of this study) is thus younger than the eastern domain (ca. 3.6 – 3.1 Ga.) (Poujol et al., 2003). Accretion along the northern edge of the growing Craton most likely caused deformational structures within the basement lithologies that could subsequently influence groundwater movement. Furthermore, the northern domain of the Kaapvaal Craton also experienced magmatic activity during early Neoarchaean times, including the emplacement of largely post-tectonic granitoids in the Pietersburg and Murchison areas (Poujol et al., 2003). The following sections consider the various Archaean subdomains within the study area, and then consider some of the supracrustal successions which are preserved above these basement rocks, and which border the study area.

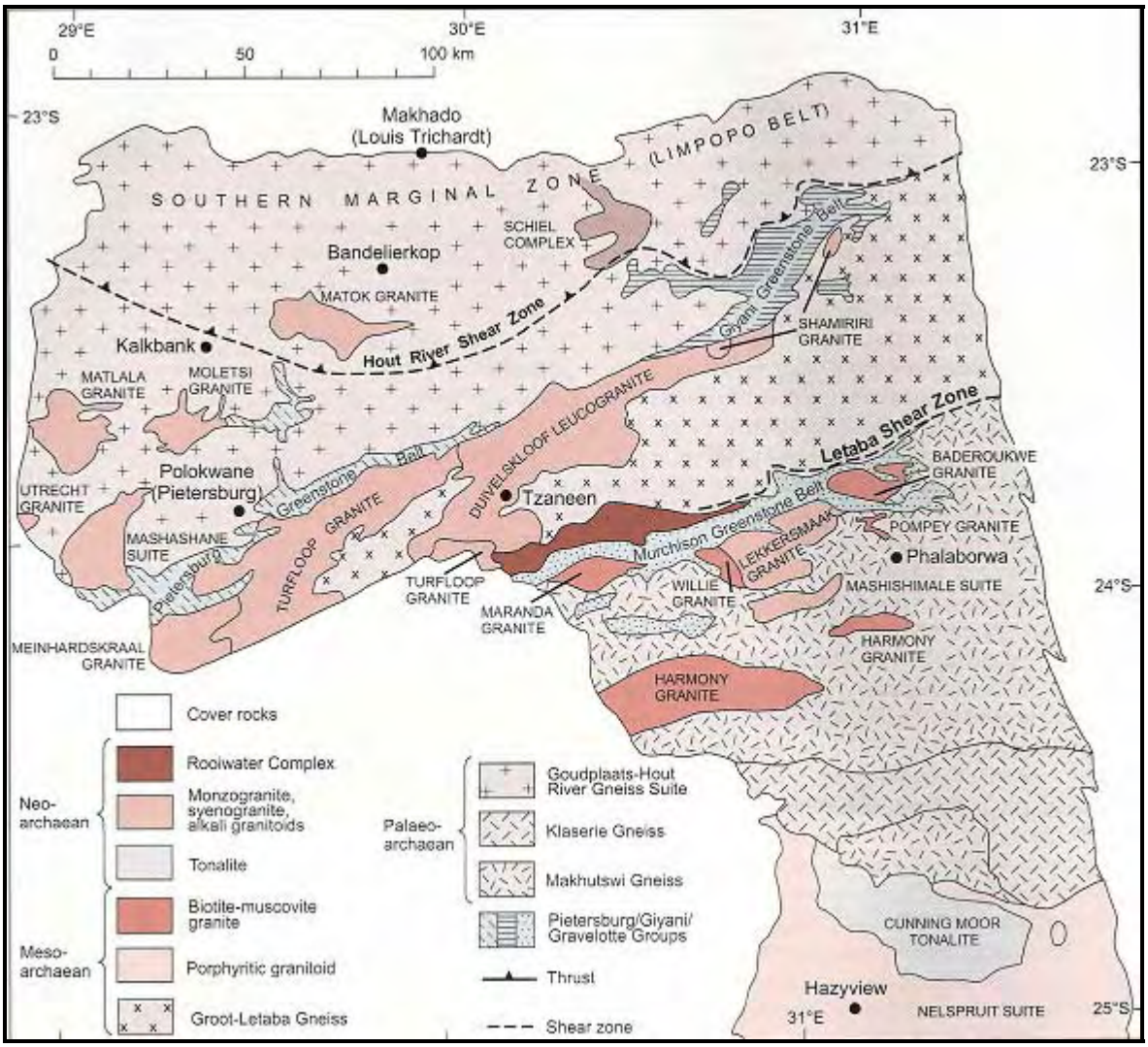

Figure 5: Map of the northern and north-eastern sectors of the Kaapvaal Craton and their different granitoid occurrences (from Robb, et al., 2006)

2.1.3. Paleoarchaean Intrusions (3600 – 3200 Ma) and the Pietersburg- and Giyani Greenstone Belts:

The Pietersburg and Giyani Granite-Greenstone Belts extend parallel to, and to the south of the Southern Marginal Zone (SMZ) of the Limpopo Belt and are separated by a 60km wide zone of intensely migmatised rock. Anhaeusser (1992) suggests that these two belts are actually parts of the same Granite-Greenstone Belt, with their tectono-thermally reworked equivalents and associated granitoids between them. Kröner et al. (2000) on the other hand, regard the Giyani and Pietersburg Granite-Greenstone Belts as two separate crustal units, which were originally in close proximity to one another, but were later displaced by strike-slip movement.

The NE-trending Pietersburg Greenstone Belt (PGSB) is made up of two well-defined tectonostratigraphic units that are separated by an unconformity (De Wit et al., 1992). Locally, evidence for northwest-verging thrust movement between these two units has also been found. The lower unit is a typical greenstone sequence with a Pb/Pb age of 2.4 Ga. (Barton, 1990), whereas the upper unit, called the Uitkyk Formation, is an arenaceous to rudaceous unit that can be correlated with the Central Rand Group of the Witwatersrand Basin (de Wit et al., 1992). Terrain accretion along the northern margin of the Mid-Archaean protocraton resulted in northward-verging thrusts along the PGSB (de Wit et al., 1993). The 3203,3 Ma ± 2,0 Ma Giyani Greenstone Belt also trends NE, and is surrounded by pre-3200Ma polydeformed gneisses (Kröner et al., 2000).

Apart from the greenstone belts, the northeastern section of the Kaapvaal Craton (North of 25°S) consists of various other Archaean subdomains. Of importance to the present study are the Paleoarchaean intrusions (3600 – 3200 Ma) that underlie a large part of the study area. Dominating the northern half of the study area is the Goudplaats-Hout River Gneiss Suite (GHGS). A wide variety of granitoid gneisses varying in type and composition belong to this suite which is found both north and south of the Hout River Shear Zone. Most of the phases of the GHGS have emplacement ages of around 2900Ma and seem to have been generated by dehydration melting of amphibolites and biotite gneiss protoliths (Robb et al., 2006).

Throughout this major magmatic period, various gneiss precursors extensively pervaded an older granitoid crust, of which only minor leftovers in the form of *c.*3300 Ma dark grey gneisses remain today. This crustal material also yields an age older than its neighbouring greenstone belts, which suggests that it served as a basement for the greenstone belts or represents a separate crustal block adjacent to the greenstones. Two main types of gneiss are found in the Lowveld, South of the Murchison Greenstone Belt (MGSB). Firstly, the layered composite Makhutswi Gneiss extends for 60km south of the MGSB and also south of the Klaserie Gneiss. Karoo and Transvaal sediments cover the Makhutswi Gneiss in the east and west respectively. The Makhutswi Gneiss is complexly folded, and in some areas intruded by a younger, unmigmatised biotite gneiss of tonalitic composition. These younger local intrusions are Mesoarchaean in age. At the northern boundaries of the Cunning Moor Tonalite and the Nelspruit suite lies a 30km wide E-W stretching strip of “homogeneous” gneiss called the Klaserie Gneiss. Mineralogically, the Klaserie gneiss is similar to the Makhutswi Gneiss, but appears to be relatively younger than the latter. Furthermore, the Klaserie Gneiss is well foliated.

2.1.4. Mesoarchaean Intrusions (3200 – 2800 Ma) and the Murchison Greenstone Belt (MGSB):

The Murchison Greenstone Belt exists along a major ENE-WSW crustal lineament that can be traced all the way to Thabazimbi, known as the Thabazimbi-Murchison Lineament (TML). This is a 400km+ long, poly-deformational zone with a width of about 25km (Vearncombe et al., 1991). The TML was an important control on the spatial deposition or emplacement of later successions such as the Wolkberg Group, Transvaal Supergroup, the Bushveld Igneous Complex and the Waterberg Group. Because of the sub-parallel orientation of the TML and the Limpopo Belt, one expects a number of geological structures in the study area to be parallel to this ENE-WSW trend. Vearncombe et al. (1992) interpreted the MGSB as the deformed remnants of five distinct domains that have been tectonically juxtaposed. Two of these domains were Archaean island arcs which obducted onto the proto-Kaapvaal Craton (Vearncombe et al. 1991). The MGSB is bounded by granitic gneisses, migmatites and pegmatites (discussed below). Dating of the MGSB revealed an age of 3090-2970 Ma. (Brandl et al., 1996; Poujol et al., 1996).

The oldest magmatic event in the vicinity of the MGSB led to the formation of a batholith-shaped intrusion called the Harmony Granite. This poorly exposed intrusion is mainly made up of light-grey, coarse-grained granite with a locally developed porphyritic variety (Poujol and Robb, 1999). On the eastern side of the MGSB lies the Baderoukwe Granite. Although various phases exist within the Baderoukwe Granite, its main phase has a granodioritic character and is slightly peraluminous. Both the Baderoukwe- and the Willie Granites show signs of strong marginal deformation orientated parallel to the MGSB contact, which might indicate a late solid-state rise of granite juxtaposed against the denser greenstone lithologies (Annaeusser, 1992). It is believed that granite magmatism was associated with volcanism at about 2970 Ma., since the Discovery Granite on the southern edge of the MGSB yielded an age of 2969 ± 14 (Poujol, 2001). Another relatively small Mesoarchaean intrusion adjacent to the southern edge of the MGSB is the Willie Granite. This medium-grained granite is grey, with microcline megacrysts of 3cm and longer and formed at a time of major felsic magmatism on the Kaapvaal Craton between 2820 and 2880 Ma (Robb et al., 2006).

Groot Letaba Gneiss is a collective term, which refers to all the granitoid gneisses between the MGSB and the Pietersburg-Giyani greenstone belts (Brandl and Kröner, 1993). The Groot Letaba Gneiss includes a wide variety of closely fused gneisses including fine- to medium-grained tonalite, coarse-grained trondhjemite and minor banded and linear gneisses. The rocks have a massive appearance in some cases, but are well- to weakly-foliated and strongly folded for the most part, though the

orientation of folds is not mentioned in literature. Gneisses belonging to this unit are generally migmatised with leucosome bands belonging to distinct generations of magma. Small inclusions of mafic to ultramafic greenstone are found in some areas, implying the intrusive nature of the gneiss protolith with the greenstone belt. Various generations of gneisses are represented by the Groot Letaba Gneiss, one of which is the gneiss near Tzaneen and further west, which yielded Pb-Pb ages of *c.* 3100-3000 Ma (Robb et al., 2006). The Pietersburg Greenstone Belt is intruded by two strongly foliated granitoid bodies. Firstly, by the trondhjemitic Melkboomfontein Gneiss which represents one of the youngest, strongly foliated granitoids at *c.* 2853 Ma. and secondly by the tonalitic Mosokgome Gneiss (Kröner *et al*., 2000).

2.1.5. Neoarchaean Intrusions (2800 – 2500 Ma):

During Early Neoarchaean times magmatic activity caused largely post-tectonic granitoid emplacements in the Pietersburg and Murchison areas. Neoarchaean granites generally form prominent topographic features in the study area, relative to the older granitoid gneisses (Robb et al., 2006). The ages of these intrusions range from 2800 Ma (upper limit dated from regional deformation of surrounding rocks upon emplacement) and 2650 Ma (lower age limit of Transvaal Supergroup strata that overlie the intrusions) (Kröner *et al*., 2000).

Of the Neoarchaean intrusions associated with the Pietersburg and Giyani Greenstone Belts, the Turfloop Granite is the largest and best studied. The Turfloop Granite trends roughly NE-SW along the southern border of the PGSB and ranges in composition from granodioritic to monzogranitic, which might be an indication that it is composed of a number of smaller plutons (Henderson *et al.*, 2000; Kröner *et al*., 2000). The Meinhardskraal Granite has intruded to the southwestern side of the Turfloop Granite. Compositionally, the different phases of the Meinhardskraal Granite vary between monzogranites, syenogranites and alkali granites (with alkali feldspar megacrysts showing a strong north-easterly preferred orientation) (Robb et al., 2006).

At the south-western end of the PGSB the Mashashane Suite batholith intrudes the Goudplaats-Houtriver Gneiss Suite. The Mashashane suite consists of three distinct phases, called the Lunsklip, Uitloop and Uitvlugt Granites (Brandl, 1985, 1986, in press). All three of these phases contain blue opalescent quartz (De Villiers and Brandl, 1977). The Uitvlugt Granite is the oldest of these three intrusions, while the Lunsklip Granite is the dominant phase. Uitvlugt and Lunsklip Granites are both metaluminous, whereas the Uitloop Granite is slightly peraluminous (Robb et al., 2006). Due to the distribution of its three phases, the Mashashane Suite could represent a large sheet-like intrusion with a shallow southwesterly dip.

One of the few S-type Neoarchaean granites in the northern part of the Kaapvaal Craton is the Utrecht Granite. This tabular sheet that tilts gently to the west is a medium to fine-grained, pink, leucocratic rock with a local pink pegmatoidal variety. It is believed that the Utrecht Granite formed by partial melting of a largely pelitic protolith under granulite grade conditions (Robb et al., 2006).

North of the Mashashane Suite lies the Matlala Granite, an almost circular batholith composed of various phases (Brandl, 1986). The two most common phases include a fine-grained, pink granite and a medium-grained porphyritic, pink granite. A prominent off-shoot of the Matlala Granite, called the Chloe Dyke, possibly formed in a pre-existing zone of weakness in the country rock.

East of the Matlala Granite Lies a batholith of similar size called the Moletsi Granite, which is made up of three phases (Brandl, 1985, 1986, in press). In the core of the body, a coarse-grained pinkish to pinkish-grey rock occurs. Around the central phase is a younger, grey to pinkish grey, coarse-grained variety. Both of these phases contain rafts of the initial fine-grained, dark grey, tonalitic granite. Analogous to the Matlala Granite, the Moletsi granite also has prominent off-shoots trending in a northerly direction (Robb et al., 2006).

Just north of the Hout River Shear Zone (in the Southern Marginal Zone of the Limpopo Belt) the Matok Granite is located (Brandl, 1985, 1986). The Matok Granite is unique amongst granitic bodies in the northern part of the Kaapvaal Craton in that it contains a large charnockitic component (mainly found in the northern part of the Matok Granite). Several NE-trending shear zones run through the Matok Granite. The older charnockitic suite contains enderbite and charno-enderbite, whereas the younger granitic suite comprises up to eleven different phases (Barton et al., 1992; Bohlender, 1992). Roughly 20km northwest of the Matok Pluton is the Hugomond Granite. This relatively small granite from *c.* 2658 ± 2 Ma is coarse-grained grey biotite granite which is porphyritic in areas and cut by tourmaline-bearing pegmatite veins (Robb et al., 2006).

Two distinct intrusive stocks on the southern and eastern side of the Giyani Greenstone Belt are referred to as the Shamiri Granite (Vorster, 1979; Brandl, 1987). At both localities, the Shamiri Granite is a grey, medium-grained rock, which can grade into a coarse porphyritic phase with microcline megacrysts of up to 6cm. Since rotated rafts of Shamiri Granite are found within the Duiwelskloof Leucogranite, the former predates the latter. The Duiwelskloof Leucogranite is a large, northeast-trending, elongate intrusion that stretches from the southeastern boundary of the Giyani Greenstone Belt to the Turfloop Granite. The northern boundary of the Duiwelskloof Leucogranite is

fairly linear (same orientation as the two adjacent greenstone belts) and may exploit a tectonic lineation. Dehydration melting of a pelitic source at a relatively shallow crustal level is believed to have been the method of formation of this peraluminous S-type granite (Robb et al., 2006).

Small plutons and dykes of the Palmietfontein Granite probably represent the youngest granitic rocks north of the Pietersburg Greenstone Belt in South Africa, with a Rb-Sr whole rock age of 2456 ± 78 Ma (reported by Barton *et al.*, 1983). Palmietfontein Granites are unfoliated and mainly fine- to medium-grained pinkish grey granodiorites.

There are a number of Neoarchaean granitoids south of the Murchison Greenstone Belt. First of all, the Vorster Suite is emplaced along the southern Boundary of the MGSB in an area where many ovoid granite bodies form an intricate pattern with intervening greenstone nodules (Brandl, 1987; Walraven, 1989; Vearncombe *et al.*, 1992). Originally, the suite was defined as comprising the following four phases: Lekkersmaak-, Willie-, Pompey- and Baderoukwe Granites. Of these four granites, the Lekkersmaak Granite has the largest aerial extent. The Lekkersmaak granite is a grey, medium-grained rock, which becomes coarser towards its centre and also contains common porphyritic types. Recently, the Willie Granite yielded a Mesoarchaean age older than 2800 Ma (Poujol and Robb, 1999; Poujol, 2001) and is therefore no longer considered a part of the Vorster Suite magmatic event. Contacts between the Willie- and Lekkersmaak Granites that outcrop are sheared and therefore relative age relationships are hard to determine. Several small stock-like bodies away from the main batholith make up the Pompey Granite. This medium-grained granite varies from light grey to pink and can be classified as a syenogranitic rock.

Slightly south of the Vorster Suite a narrow northeast-trending intrusion called the Mashimale Suite occurs (Brandl, 1987; Walraven, 1989; Vearncombe *et al*., 1992). The Hoed-, Lillie- and Transport Granites are the three phases of this suite. Lillie- and Transport Granites are medium- to coarse-grained stock-like intrusions. The Hoed Granite is a fine-grained, locally porphyritic biotite granite that is intruded by the other two minor phases. A ductile shear zone with apparent sinistral displacement exists near the northern margin of this intrusion.

Apart from the Duiwelskloof Leucogranite and the Utrecht Granite, the other massive granites are regarded as I-type granites (based on the limited geochemistry), which formed in subduction collision-related settings. However, one could argue that these granites actually represent A-type anorogenic granites, as they are not foliated nor

metamorphosed. Heat necessary for such granites to form could have been supplied by under- and intraplating of mantle-derived gabbroic magmas (Robb et al., 2006). Bordering the Murchison Greenstone Belt to the north is a layered mafic igneous body called the Rooiwater Complex. This complex is capped by a 2740 ± 4 Ma (Poujol *et al*., 1996) hornblende tonalitic rock. Rooiwater Complex rocks mainly consist of albite and large, opalescent blue quartz grains. Furthermore, minor opaque minerals and secondary blue-green hornblende, chlorite, epidote, piemontite and muscovite are also present. Van Eeden *et al.* (1939) believed that the Rooiwater Complex is the late-stage differentiate of underlying gabbro-anorthosite of the Novengilla Suite.

The only tonalitic "late" pluton in Mpumalanga is the Cunning Moor Tonalite, which intrudes gneisses and migmatites of the Nelspruit Suite. It is a 50km-long oval shaped body, consisting predominantly of grey, medium-grained, massive, homogenous tonalite (Robb, 1978; 1994).

2.1.6. The Limpopo Belt (LB):

The Limpopo Belt (LB) in the northern part of South Africa may be the oldest example of a Himalayan-type continent-continent collisional orogeny between large cratons. This granulite-grade metamorphic belt has an ENE trend and stretches for approximately 550km with a width of 250km (Bumby & van der Merwe, 2004). Although there is some dispute over the timing of the Limpopo orogeny, a general consensus has been reached by most geologists over its formation mechanism. The orogenic event occurred as an oblique collision between the northern edge of the Kaapvaal Craton and the southern edge of the Zimbabwe Craton, with a third exotic terrain encorporated into the orogen, preserved between the two cratons. The combination of the Kaapvaal and Zimbabwe cratons is referred to as the Kalahari Craton.

The resulting LB consists of three main crustal zones, namely the Northern Marginal Zone (NMZ), the Central Zone (CZ) and the Southern Marginal Zone (SMZ), which lie parallel to one another in an ENE direction (refer to Figure 6). The NMZ represents the metamorphosed southern margin of the Zimbabwe Craton. To the north, the NMZ is bounded by the Northern Marginal Shear Zone, whereas the shallow south-dipping Triangle and Magogaphate Shear Zones separate the NMZ from the CZ in the south. At the southern boundary of the CZ lies the Palala Shear Zone and Tshipise Straightening Zone, which dip steeply to the north. The Triangle and Palala shear zones have dextral and sinistral senses of shear respectively (McCourt & Vearncombe 1987), suggesting that the CZ may have been emplaced as a westwards-vergent nappe. South of the Palala Shear Zone lies the SMZ, that in turn is bounded further south by the northwards-dipping Hout River Shear Zone. The Hout River Shear Zone incorporates the ortho-

amphibole isograd in its hanging wall, so that relatively low-grade basement rocks to the south are separated from higher amphibole- and granulite-grade rocks in the SMZ hanging wall. A large part of the area investigated in this study falls within the SMZ, which can be readily recognized by the presence of several ultramafic bodies, which are absent in the Kaapvaal Craton lithologies in the footwall.

When viewed in a N-S cross section, the LB appears to be a very symmetrical feature, apart from the fact that the Palala Shear Zone dips much steeper than the Triangle Shear Zone. Another symmetrical pattern within the LMB is indicated by metamorphic grades that show a general increase from the marginal zones (amphibolite facies) towards the CZ (granulite facies).

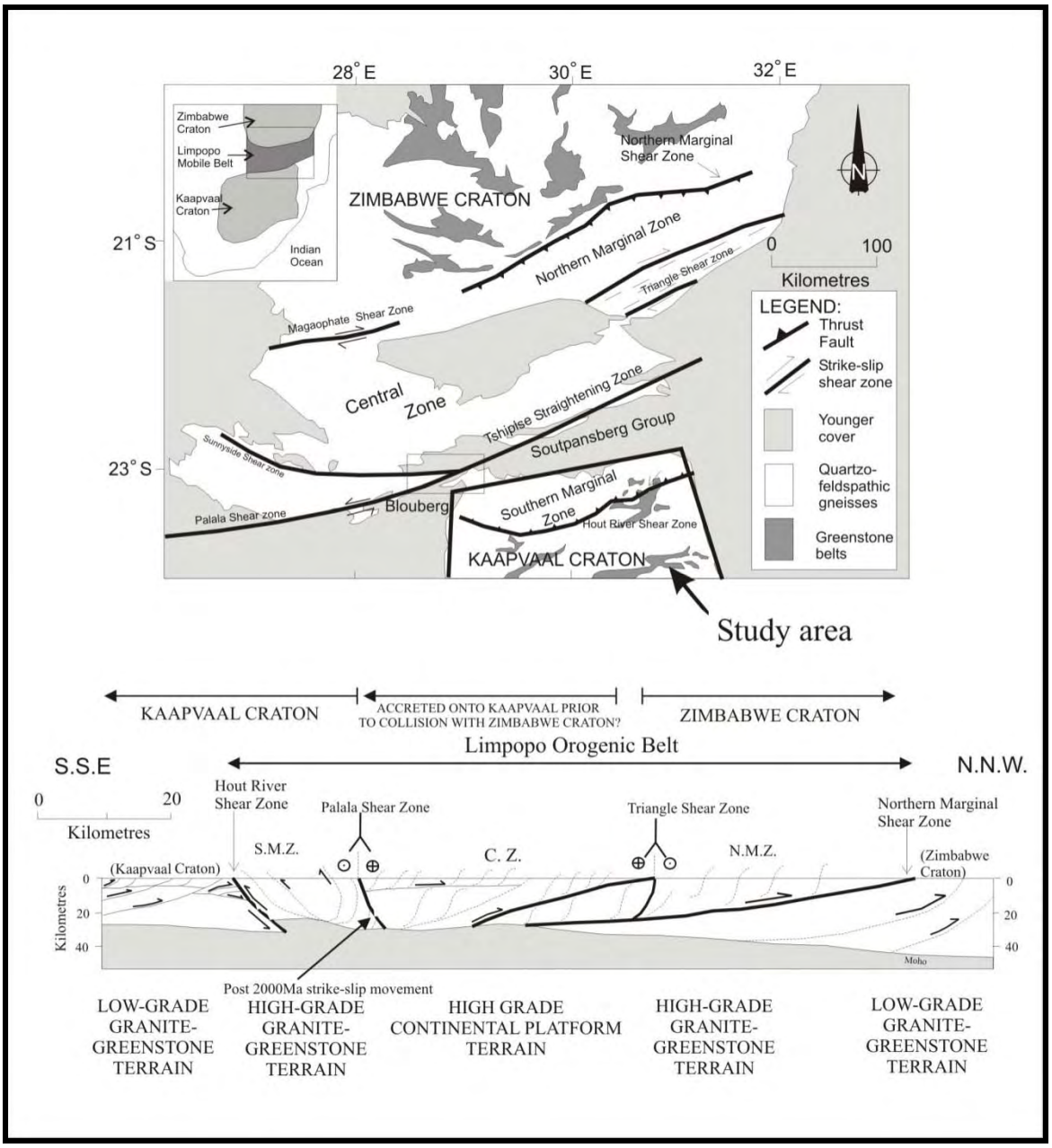

Figure 6: Regional geological map and cross section through the Limpopo Belt, showing the subdivisions, major shear zones and location of northern part of the study area (modified after Bumby & van der Merwe, 2004).

2.1.7. Timing of the Limpopo Orogeny:

Two main interpretations concerning the timing of the Limpopo Orogeny have been made in the past. The first interpretation focuses on the age of granitic gneiss bodies within the CZ. These granitic bodies, such as the Bulai Gneiss, are believed to have intruded into the Beit Bridge Complex as a result of decompression melting during exhumation, following the Limpopo collisional event (Bumby & van der Merwe, 2004). Dating of the Bulai Gneiss gives an indication of the minimum age of the collision at about 2.57 – 2.66 Ga. (McCourt & Armstrong, 1998). Further studies have been done

around the Blouberg area (e.g. Bumby et al., 2004), which is located along the projected strike of the Palala Shear Zone. In this area, lithologies from the Blouberg Formation, Waterberg and Soutpansberg Groups are found above a nonconformity with the granulite-grade gneiss of the LB and are separated from one another by angular unconformities. Due to this long tectono-sedimentary record in the Blouberg area (from the Limpopo collisional event up to the deposition of the Soutpansberg strata 1.97 - 1.8 Ga.) an Archaean-aged (ca. 2.6 - 2.7 Ga.) collision is favoured. Structures recorded by Bumby et al. (2004) in the Blouberg area reflect a southward-vergent tectonic event at ca. 2.0 Ga. According to this model, the ca. 2.0 Ga. event is interpreted as a reactivation of the Palala Shear Zone, rather than the primary Limpopo collision itself.

A second model concerning the timing of the Limpopo Orogeny deals with dates derived from metamorphic silicates found in the Triangle and Palala Shear Zones, as well as anatectic melts from the CZ. According to Holzer et al. (1998) and Schaller et al. (1999), these silicates and melt components represent times of peak metamorphism, thus implying the actual time of the collision between the KVC and the ZC. According to this model, a Proterozoic (ca. 2.0 Ga.) primary collision is suggested.

2.1.8. The Hout River Shear Zone (HRSZ):

One of the potential structural targets for groundwater in the study area is the Hout River Shear Zone (HRSZ). The HRSZ is located on the southern side of the Limpopo Belt (LB) and forms the boundary between the low grade basement lithologies of the Kaapvaal Craton (KC) and the higher grade rocks of the Southern Marginal Zone (SMZ). A lot of similarities exist between the HRSZ and its northern counterpart, the Northern Marginal Shear Zone (NMSZ), which separates the Zimbabwe Craton (ZC) from the Northern Marginal Zone (NMZ). However, the HRSZ is generally more steeply inclined than the NMSZ (Smit et al., 1992). In general the HRSZ comprises E-W striking, steeply northward-dipping thrusts and reverse faults, as well as several NE-SW striking strike-slip faults (Smit et al., 1992). The strike-slip faulting on the eastern part of the HRSZ changes to a system of frontal and lateral ramps as one move to the western section (refer to Figure 6). Geothermobarometric studies have shown that the vertical displacement of the HRSZ was of the order of 15km (Miyano et al., 1992; Perchuk et al., 1996).

Prior to the formation of the HRSZ, north-vergent thrusting ($\mathbf{D_1}$) took place along moderately southward-dipping thrusts in the northern margin of the KC. Through lead stepwise leaching (PbSL) of titanite from the Renosterkoppies Greenstone Belt in the KC, Passeraub et al. (1999) have shown that this initial event ($\mathbf{D_1}$) took place between 2760 and 2710 Ma. This first event was followed by amphibolite facies southward-vergent

thrusting ($\mathbf{D_2}$) along the newly formed HRSZ. The $\mathbf{D_2}$ event is characterized by cooling and decompression to amphibolite facies conditions. Such conditions led to the exhumation of the charno-enderbitic rocks of the ($\mathbf{D_2}$) Matok Pluton along the Matok Shear Zone, which forms part of the HRSZ. Ductile reactivation of the Matok Shear Zone postdates the emplacement of granodioritic members of the Matok Pluton, which implies that $\mathbf{D_2}$ thrusting continued after the exhumation to mid-crustal levels. According to Kreissig et al. (2001), the geochronology of the HRSZ stretches over ~90Ma (c. 2690 until 2600 Ma.) of episodic shearing. Lastly, strike-slip shear zones parallel to $\mathbf{D_2}$ structures may indicate a continuous transition from high grade $\mathbf{D_2}$-shearing to mylonitic $\mathbf{D_3}$. Metapelites of the Bandelierkop Formation are only found in the SMZ, north of the HRSZ. Furthermore, the distribution of swarms of dolerite dykes also seem to be influenced by the HRSZ, as these are more densely populated south of the HRSZ, in low-grade rocks of the KC, and are less common within the SMZ.

The mylonitic rocks which occupy the HRSZ are likely to be more highly weathered than the adjacent gneisses and granites of the area. Such predicted deep weathering profiles along the HRSZ are expected to have a strong positive influence on the hydraulic conductivity parallel to the strike of the shear zone. Unfortunately, faults can also lower an area's water table by acting as drainage pathways (Mulwa *et al*., 2005).

2.1.9. Dolerite dykes:

Dyke swarms outcrop more densely in the north-eastern domain of the Kaapvaal than elsewhere on the craton and northeast-striking diabase dykes are dominant in the study area. From their orientation and age, these northeast-striking dykes are associated with 2.7 Ga. Ventersdorp Supergroup trends (Uken & Watkeys, 1997), which formed either in response to the Limpopo orogeny (Burke et al., 1985) or by crustal extension due to mantle plume activity (Hatton, 1995). Later Karoo dolerites sporadically cut through the older dykes but usually follow the same intrusion paths as their Archaean predecessors. One of the possible controls of the dyke emplacement in the studied area is the Hout River Shear Zone (HRSZ), because many more dykes are observed north of the HRSZ (in the SMZ) than south of it.

In groundwater exploration one should not only consider the orientations of dykes, but also their thickness. Pumping tests in Botswana revealed that dolerite dykes thicker than 10m serve as groundwater barriers, whereas those that are narrower tend to be permeable due to the fact that cooling joints and fractures are developed in them (Bromley *et al*., 1994). Geometry, grain size and the degree of weathering are other factors which, through a complex interplay, affect the hydraulic conductivity of dolerites. However, due to the structural geological nature of this thesis, the author

largely focussed on the orientation and distribution of dolerites and their associated joints. Stettler *et al*. (1989.) divided the northern part of South Africa into six domains based on the character and orientation of their magnetic lineaments. Domains A, C and E are similar in character in that they have the highest frequency of magnetic lineations and a high degree of NE-SW to ENE-WNW orientation. Domains B and D on the other hand have more randomly orientated magnetic lineations (refer to Figure 7).

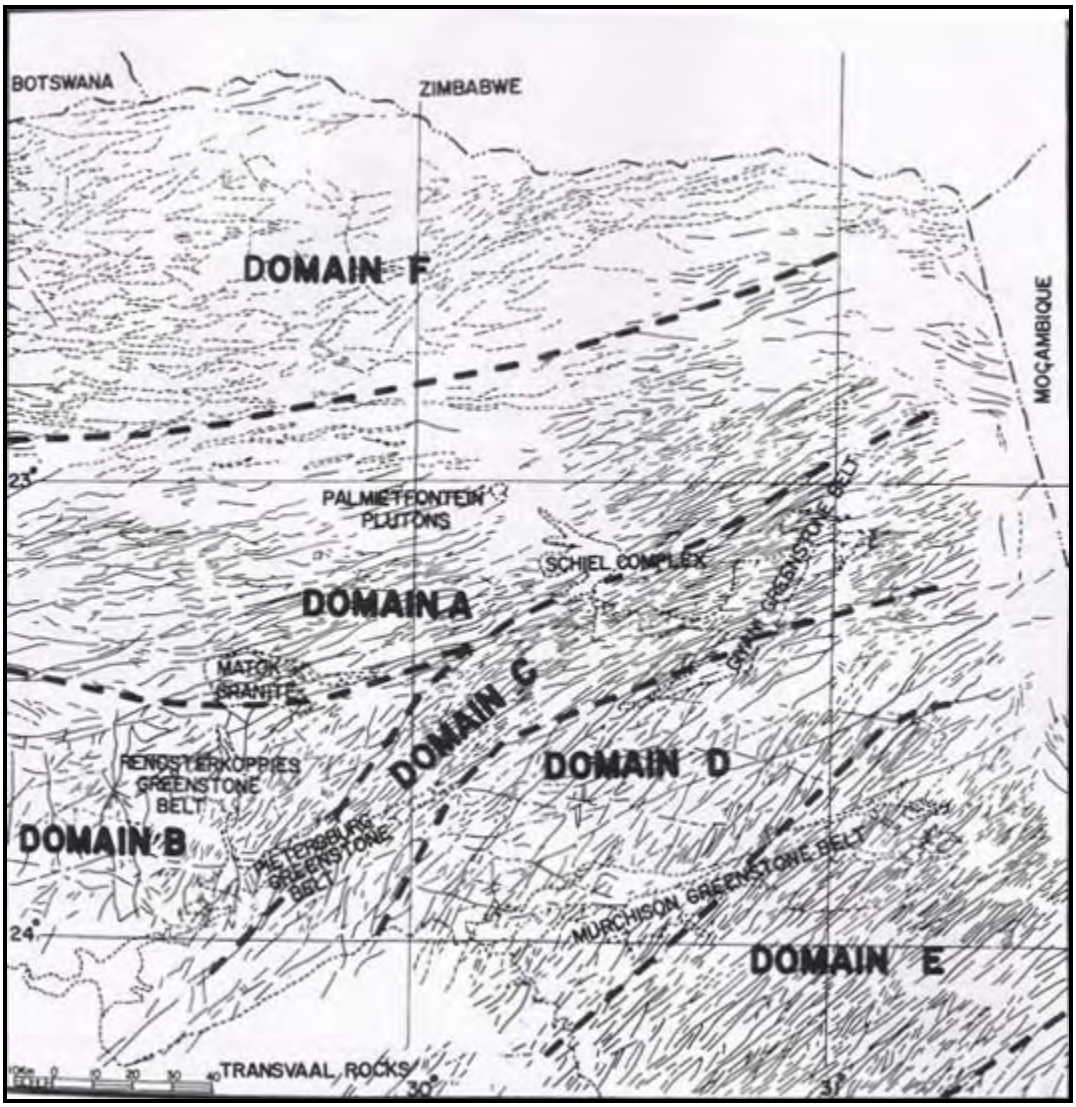

Figure 7: Aeromagnetic lineament map of the northern part of South Africa an interpreted lineament domains (after Stettler et al., 1989).

2.1.10. Wolkberg Group:

The Wolkberg Group is an up to 2000m thick sedimentary succession (Button, 1973, Bosch, 1992), which outcrops along the southern border of the study area. It consists of alternating feldspathic quartzites and argillaceous sedimentary rocks, coarse quartz arenites, some conglomerates, basaltic lava and minor stromatolitic carbonate beds

(Button, 1973; Bosch 1992). The Wolkberg Group comprises, from the base upwards, the Sekororo, Abel Erasmus, Schelem, Selati, Mabin and Sadowa formations (Button, 1973; Bosch, 1992). The basal Sekororo Formation nonconformably overlies Archaean basement of the Kaapvaal craton (Button, 1973).

2.1.11. Bushveld Igneous Complex:

The western edge of the study area is bound by the northern limb of the c. 2.06 Ga. Bushveld Complex. This is a large economically important layered intrusive complex, comprises of the lower Rustenburg Layered Suite which underlies the Lebowa Granite Suite and the Rashoop Granophyre Suite, which intruded into the basement gneiss. The northern edge of the northern limb of the Bushveld Complex appears to abut against the HRSZ and the extent of intrusion may thus, in part, be controlled by such pre-existing structures.

2.1.12. Blouberg Formation:

The Blouberg Formation is a clastic sedimentary sequence that was deposited nonconformably over the granulite-grade gneisses of the LB in the far north-west of the study area. Outcrops of the Blouberg Formation are found on the eastward extension of the Palala Shear Zone, WSW of the Soutpansberg. According to Bumby et al. (2002) the depositional environment of the Blouberg Formation was most likely a deep, localized pull-apart basin caused by strike-slip reactivation along the Palala Shear Zone. Other features, like the ENE-trending Melinda Fault also affected the geometry of the Blouberg Formation. The maximum thickness of the Blouberg Formation is about 1400m (Bumby et al., 2001) of which the lower member makes up about 600m.

Lower member lithologies of the Blouberg Formation vary from coarse arkosic sandstone and channel fills of arkosic granulestone (presumably from braided streams). According to Bumby et al. (2001), the sizes of lower member sets of trough cross bedding decrease upward. Upper member lithologies of the Blouberg Formation were deposited in alluvial fans, and consist of feldspathic sedimentary breccia and conglomerate. Syn-sedimentary tectonism recorded in the Blouberg Formation is thought to reflect a 2.0 Ga. southward-verging reactivation event of the Palala Shear Zone (Bumby et al., 2004). This same southward-verging compressional event caused E-W-trending folds and locally overturned strata with reverse faults that dip to the north.

2.1.13. Waterberg Group:

The Waterberg Group similarly outcrops along the north-western margin of the study area, and consists of the Setlaole, Makgabeng and Mogalakwena formations. The basal Setlaole Formation rests nonconformably on the basement rocks, and is composed of

coarse granulestone and is locally conglomeratic. This formation is interpreted to have been deposited in a fluvial, braided river environment. The Makgabeng Formation was likely to have been deposited conformably on the Setloale Formation, and consists of large-scale trough and planar cross-bedded fine- to medium-grained sandstone, which is interpreted as an aeolianite (Bumby, 2000). The Mogalakwena Formation, in contrast, lies disconformably above the Makgabeng Formation, and further to the north rests on the Blouberg Formation on a sharp angular unconformity. These strata consist of interbedded sheets of granulestone and conglomerate in proximal areas, grading into trough cross-bedded granulesotnes and sandstones in distal areas to the SW (Bumby, 2000).

Disputes have occurred in the past over the relative age relationship between the Waterberg and Soutpansberg Groups. Basement-derived clasts were observed in the basal Tshifhefhe Formation of the Soutpansberg Group, but not in the Waterberg strata and therefore Brandl (1987) believed that the Soupansberg Group predates the Waterberg Group. However, more recent studies (Bumby, 2000; Bumby et al., 2001) showed the opposite relationship between the Soutpansberg and Waterberg Groups in the vicinity of the Blouberg Formation. Bumby (2000) and Bumby et al. (2001) found that the Soutpansberg clastic strata rest unconformably on the Mogalakwena Formation of the Waterberg Group.

2.1.14. Soutpansberg Group:

Strata from the Soutpansberg Group presently outcrop in a continuous linear escarpment stretching ENE-WSW from Punda Maria in the east to Vivo in the west, and form the northern border of the present study area. Outliers of Soutpansberg rocks also outcrop further to the west, at Blouberg, Tolwe and in the Palapye area in eastern Botswana. The Soutpansberg Group is a 1.85 Ga. volcano-sedimentary sequence (Cheney et al., 1990; Barton and Pretorius, 1997).

The Soutpansberg Group consists of the basal Tshifhefhe Formation, which is only locally developed at the eastern end of the Soutpansberg basin, and is only a few metres thick. It is comprised of strongly epidotised clastic sediments, including shale, greywacke and locally-derived conglomerate (Barker et al., 2006). This is overlain by the generally volcanic Sibasa Formation. The siliciclastic Fundudzi Formation is only developed at the eastern end of the basin. It is mainly comprised of arenaceous and argillaceous sedimentary rocks, though there are rare pyroclastic horizons, and basaltic lavas are intercalated with the sedimentary lithologies close to the top of the formation (Bumby, 2000). Overlying the Fundiudzi Formation is the Wyllie's Poort Formation, composed of northward-dipping red-pink quartzite with minor pebble washes. The base

is marked by a prominent agate pebble conglomerate, and in the east minor basaltic and pyroclastic intercalations are present (Barker, 1979). Wyllie's Poort Formation reaches thicknesses of 4000m. Lastly, the uppermost unit of the Soutpansberg Group is the Nzhelele Formation, which is volcanic at the base (400m), followed by argillaceous sedimentary rocks in the middle, and arenaceous rocks at the top (Barker et al., 2006).

2.1.15. Proposed Models for the formation of the Soutpansberg Group:

A few models pertaining to the deposition of the Soutpansberg Group have been suggested, but the two main models discussed in this report are those of Jansen (1975), Bumby et al. (2001) and that of Cheney et al (1990). Jansen (1975) proposed an aulocogen or failed rift model. Bumby et al. (2002) supplement Jansen's (1975) model by proposing that the Soutpansberg sediments were deposited in an E-W stretching half-graben, which is fault-bounded to the south. Therefore, this first model proposes a syn- to post tectonic depositional environment. On the other hand the second model, proposed by Cheney et al. (1990), suggests a large cover sequence of Soutpansberg strata that were deposited pre-tectonically. According to Cheney et al. (1990), a graben, similar to that proposed by Jansen (1975) formed after the deposition of the Soutpansberg strata, thus preserving the Soutpansberg strata within a graben, rather than being deposited within a graben. Since no Soutpansberg lithologies have been found south of the Palala Shear Zone, the model by Jansen (1975) or Bumby et al. (2001) is most favoured.

2.1.16. Drakensberg Group:

The eastern margin of the study area is marked by the eastern edge of the Kaapvaal craton. This area is underlain by rocks of the Drakensberg Group (Karoo Supergroup), which comprises flood basalts and pyroclastic deposits. According to Smith et al. (1990), these basalts are Early Jurassic in age and are linked with the onset of rifting between East and West Gondwana.

2.2. Fault and joint analysis:

In order to understand the dynamics of faulting one must first grasp the basic properties of the principal stress directions in conjunction with Coulomb's Law of Failure, which states that:

$$\sigma_c = \sigma_0 + \tan\phi(\sigma_N)$$ Coulomb (1773) and Mohr (1990)

where

σ_c = critical shear stress required for faulting

σ_0 = cohesive strength of the rock

$\tan\phi$ = coefficient of internal friction

σ_N = normal stress

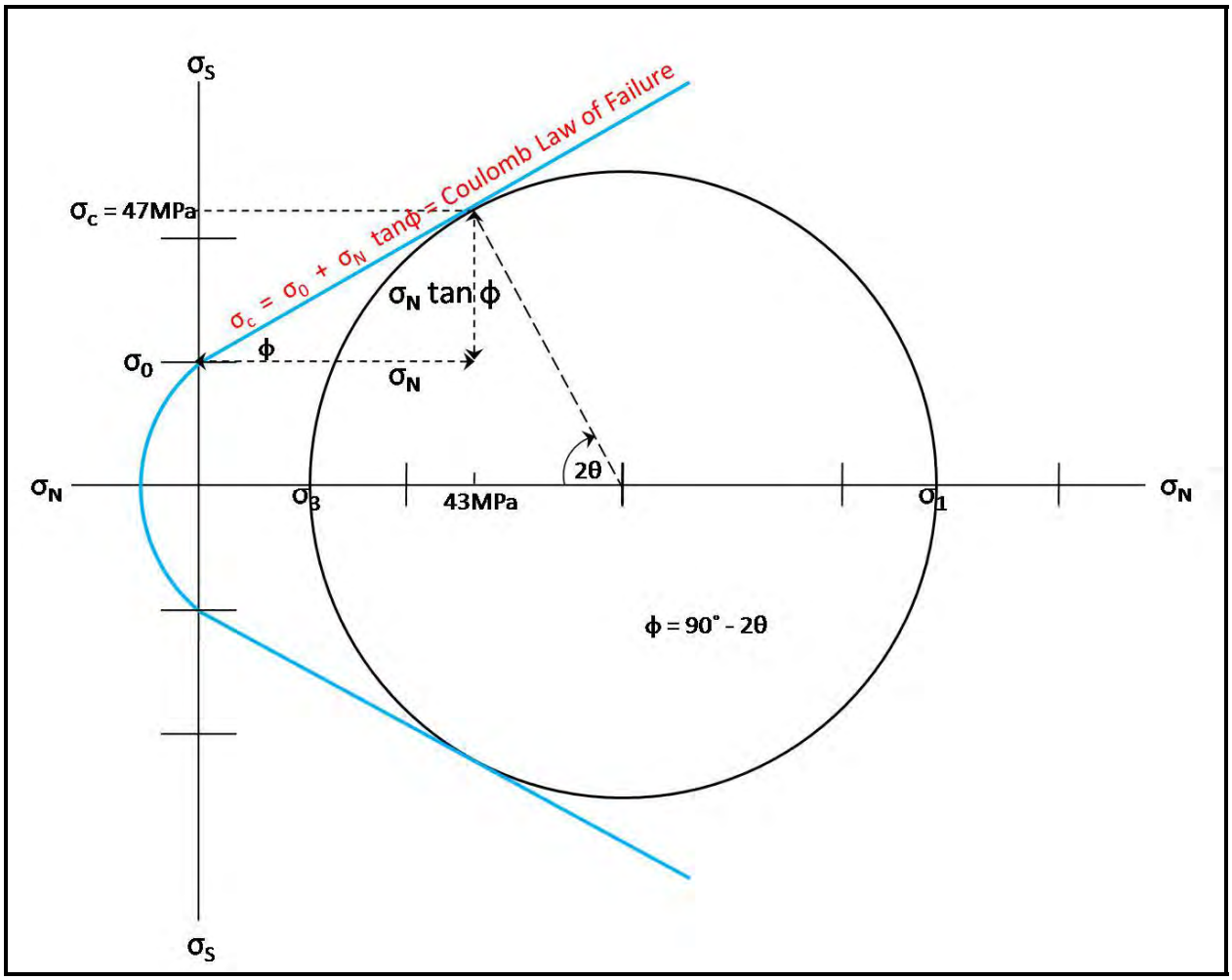

Figure 8: A Mohr diagram illustrating the principles of the Coulomb Law of Failure. Modified after Davis and Reynolds, 1996.

A rock's angle of internal friction (ϕ) determines (θ), which is the angle between the fracture surface and the direction of greatest principal stress (σ_1) (Davis and Reynolds, 1996). From the geometry of the Mohr diagram in Figure 8, one can see that

$\phi = 90^\circ - 2\theta$, therefore

$2\theta = 90^\circ - \phi$

$$\theta = \frac{90^\circ - \phi}{2}$$

Through countless laboratory tests it has been shown that most rocks possess an angle of internal friction equal to about 30˚ (Davis and Reynolds, 1996). Therefore, the value of θ is also 30˚ for most shear fractures.

Anderson (1951) realized that if one considers the Earth to be a perfect sphere, the contact between air and ground at any point on the Earth's surface forms a tangent plane along which shear stress is zero. In that case, since principal stress directions are considered as directions of zero shear stress, the surface of the Earth must be a principal plane containing two of the three principal stress directions. The third principal stress direction lies perpendicular to this principal plane so that it is vertical at any point on the surface of an ideally spherical Earth (Davis and Reynolds, 1996). Using the internal angle of friction ~30˚ as a base, together with the concept of the Earth's surface being a principal stress plane, Anderson (1951) concluded that only normal-slip, strike-slip and thrust-slip faults should be able to form at or near the Earth's surface. Normal-slip faults form when σ_1 is vertical; strike-slip faults form when σ_2 is vertical; and thrust-slip faults form when σ_3 is vertical (Davis and Reynolds, 1996). Furthermore, conjugate pairs of fault planes can form in which case the conjugate angle between such planes is bisected by σ_1. In addition to the faults already mentioned, mode I tension fractures can form parallel to the direction of principal stress (σ_1) and perpendicular to the direction of least principal stress (σ_3). Slickenside lineations are often found on fault surfaces and their orientation is defined as the intersection of the fault plane with the σ_1/σ_3 plane (Davis and Reynolds, 1996).

Strike-slip fault:

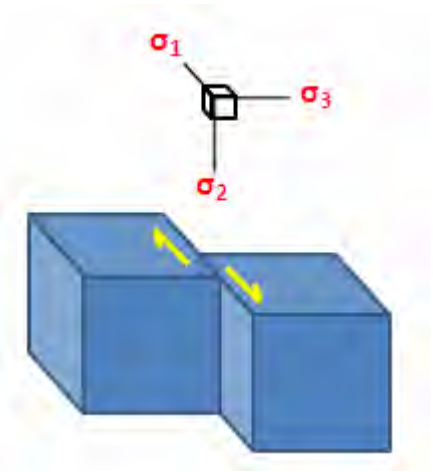

Thrust fault:

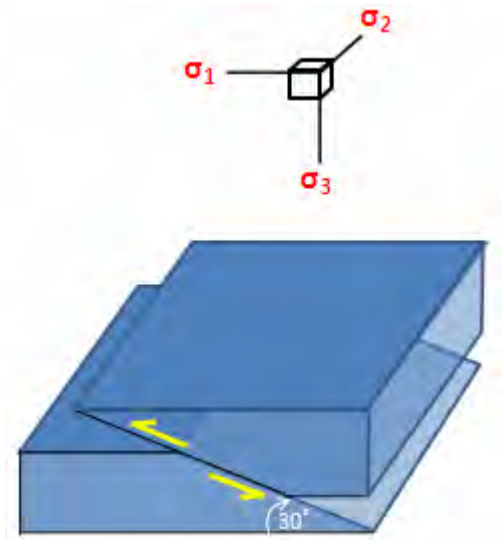

Normal- and reverse faults:

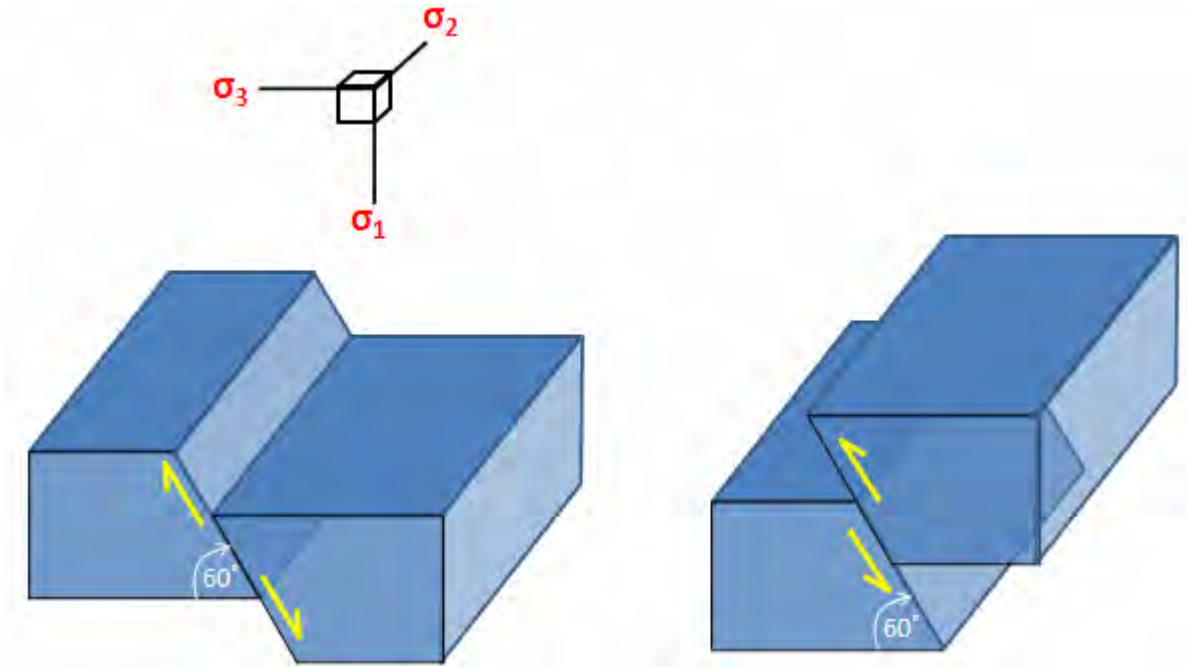

Figure 9: Illustrations of the three fault types described in Anderson's Theory, as well as a reverse fault.

PORE FLUIDS:

Since there are many more variables in nature than just the internal angle of friction and an idealistic principal stress plane, there exist a few exceptions to Anderson's Theory of Faulting and Coulombs Law of Failure. The first variable that has not been discussed yet is the existence of pore fluids at the time of faulting. Hubert and Rubey (1959) showed that high pore fluid pressure (P_f) in rocks decreases the normal stress acting on the fault/fracture plane. This lead to the modification of the Coulomb Law of Failure through the introduction of effective stress (σ^*) which is equal to the normal stress minus the pore fluid pressure. Hence, the critical stress needed to fracture a rock is also affected in the following manner:

$$\sigma_c = \sigma_0 + \tan\phi(\sigma_N - P_f)$$

At depths shallower than 3km, the fluid pressure in the Earth's crust is unconfined and equal to the hydrostatic pressure (P_h) (Twiss and Moores, 1992). Hydrostatic pressure is a function of the density of the fluid (ρ_f), the height of the fluid column (h) and the pull of gravity (g) (Davis and Reynolds, 1996).

$$P_h = \rho_f g h$$

Once below 3km, fluid pressure plays a more complex role. Due to compaction, fluid pressures are forced to occupy less and less space and therefore exceed hydrostatic pressure. To complicate matters even further, the influence of the geothermal gradient causes what is known as aquathermal pressuring. Aquathermal pressuring occurs because water has a higher coefficient of thermal expansion than rocks (Davis and Reynolds, 1996) and this phenomenon can even cause pore fluid pressure to rise to levels exceeding the lithostatic pressure (pressure derived from the weight of the overlying rock) of the host rocks (Davis and Reynolds, 1996). The fluid pressure ratio (λ) is used to describe the ratio of pore fluid pressure to lithostatic pressure:

$$\lambda = \frac{P_f}{Pl} = \frac{P_f}{\rho_r g h}$$ (Hubert and Rubey, 1959)

Elevated fluid pressures are called abnormal fluid pressures and have λ values ranging from 0.5 to 0.9, whereas hydrostatic fluid pressures' λ values range from 0.37 to 0.47 (Suppe, 1985). Abnormal fluid pressure can cause a remarkable phenomenon by forming joints at depths exceeding 10km. Formation of joints at such depths can occur in one of the following ways: 1) If the differential stress between σ_1 and σ_3 is small enough and the abnormal fluid pressure is large enough, tensional joints can form perpendicular to σ_3; 2) If

the differential stress between σ_1 and σ_3 is higher, but the pore fluid pressure remains abnormally high, transitional tensional joints can form at low angles to σ_1 (Secor, 1965). This concept is very important to this project when taking into consideration the fact that many of the basement rocks exposed at the current topographical surface of the study area originally formed at great depths.

ANISOTROPIC ROCKS:

A second variable causing deviations from Anderson's Theory is the anisotropy of rocks. If a rock contains any pre-existing weaknesses such as bedding, faults, fractures or foliation it can alter the way in which the rock reacts to stress. It has been proved that the level of critical stress required to reactivate an existing fracture plane is less than that required to fracture an unfractured sample of the same lithology (Handin, 1969). Even fractures with θ angles as great as 65˚ can sometimes be reactivated as faults (Handin, 1969). A large amount of the basement lithologies in this project's study area are foliated and therefore it is important to take note of the following exceptions to the rule: 1) If foliation lies at a small angle to σ_1, the resulting θ angle of the fracture that forms will be very small ~10˚ to 20˚. 2) If the angle between foliation and σ_1 falls between 25˚ and 45˚ the influence of internal friction can be made ineffective and fault surfaces can form right along foliation (Donath, 1961).

PRE-EXISTING FRACTURES:

As a result of its long tectonic history, the rocks in the study area have experienced many stress regimes throughout their existence. With that in mind it is obvious that pre-existing fractures were often present at the onset of a new tectonic episode. Just as in the case of anisotropic rocks, pre-existing fractures also have a deviating effect on Anderson's Theory. Byerlee's Law (1967, 1978) states that the level of critical shear stress needed for the reactivation of a pre-existing fracture is equal to the coefficient of sliding friction of the rock multiplied by the normal stress acting on the fracture plane.

$$\sigma_c = \sigma_0 + \tan\phi_f(\sigma_N)$$

This basically means that the level of stress required for the reactivation of a pre-existing fracture depends on the friction along the fracture plane and the orientation of that plane (Davis and Reynolds, 1996). Through extensive experimenting, Byerlee (1967, 1978) further concluded that except for conditions of very low confining pressure (<200MPa), friction is effectively the same for all rock types.

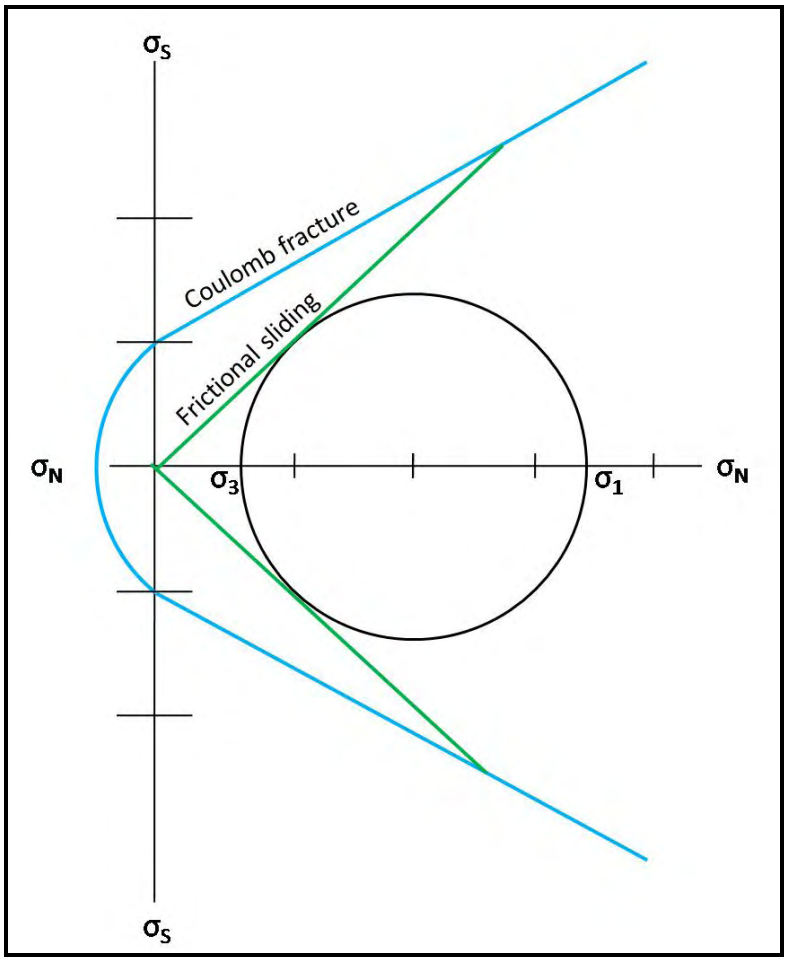

Figure 10: An illustration of the relationship between a Coulomb frictional envelope and a frictional sliding envelope on a Mohr diagram. If the differential stress circle from the stresses in a rock with pre-existing fractures touches the frictional sliding envelope on the diagram, renewed sliding will take place along the existing fractures instead of forming new fractures. Modified after Suppe, 1985.

THREE-DIMENSIONAL STRAIN:

Experiments that test rock deformation properties usually involve conditions of two-dimensional coaxial stress and strain. Under these conditions, Coulomb's Law predicts the formation of one conjugate pair of faults. However, rocks in nature have often been found with two pairs of conjugate faults (four faults). A possible explanation for the two conjugate fault pairs is simply to assume that two separate faulting events took place in the same area (Davis and Reynolds, 1996). However, Reches (1978) proved the presence of more than one fault set (pair) is often due to a single faulting event generated by a three dimensional strain field. For example, three or more fault sets arranged in orthorhombic symmetry is a characteristic fault pattern that occurs when rocks are stretched or shortened by different amounts in three mutually perpendicular directions Reches (1983) (see Figure 11). According Reches' (1983) experiments, the angular relationships among fault sets formed under these conditions depends both on the angle of internal friction (ϕ) and the ratio of strain along the principal finite stretch directions (S_1, S_2 and S_3).

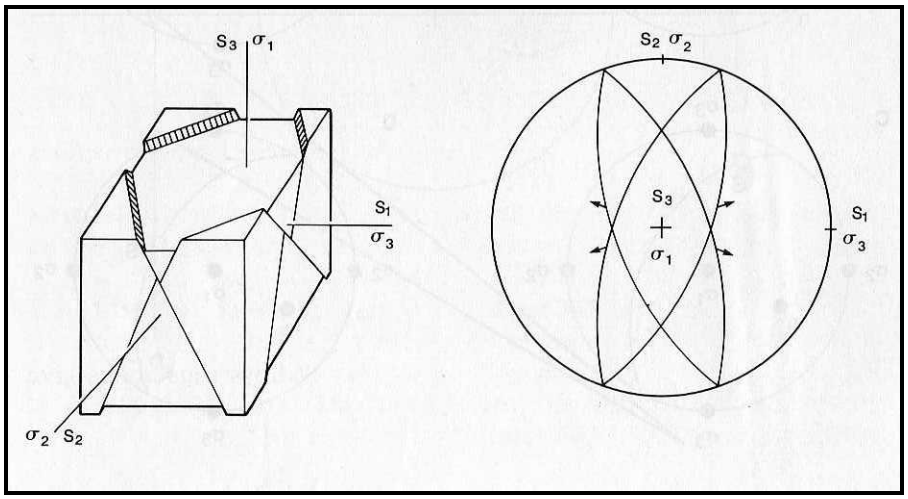

Figure 11: Two pairs of conjugate fault sets produced in a three-dimensional strain field. From Reches, 1983.

REVERSE FAULTS:

Reverse faults are formed by crustal shortening and usually dip ~60˚ or steeper. Although not uncommon, reverse faults don't fit into the typical model of Anderson's Theory. An obvious explanation for the formation of reverse faults is the reactivation of previous normal faults (Davis and Reynolds, 1996). Another explanation for the formation of reverse faults is the fact that stress trajectories become inclined or curved with depth (Davis and Reynolds, 1996). Theoretically, the dissipation of horizontal compressive stress can cause a strain field with curved stress trajectories, causing curved faults which are partly thrust faults which steepen upward into reverse faults (Hafner, 1951). On the other hand, other experiments have shown that shallow thrusts can steepen with depth to become reverse faults (Sandord, 1959).

CHANGES OF ROCK VOLUME DURING FAULTING:

A last variable that causes faults in nature to deviate from the faults described by Anderson's Theory is changes in rock volume during faulting (Aydin, 1978; Aydin and Johnson, 1978). This phenomenon usually occurs in poorly cemented, porous sandstones that can decrease in volume as a result of the collapsing of pores under stress (Davis and Reynolds, 1996) and therefore shouldn't play a role in the basement rocks of the study area. Faults that occur in unison with volume reduction are called deformation bands or band faults and often form together in zones (Davis and Reynolds, 1996).

2.3. Geological stress and strain regimes in Southern Africa:

A very interesting study was conducted by Bird et al. in 2006 regarding patterns of stress and strain rate in Southern Africa. Models were produced of deviatory stress fields, primarily caused by the following three sources: 1) lateral variations in the density moment; 2) resistance of unbroken lithosphere to the relative rotation of the Somalia Plate relative to

the African Plate; 3) stress concentration near the tips of frictionless cracks. Unfortunately, it was impossible to isolate any of these sources in a model. Given that some ancient faults in Southern Africa have been reactivated, including faults from the Limpopo Belt (Brandl, 1995; Partridge and Maude, 2000), it may take generations of research in order to encompass a full understanding of the strain rate field in this area.

In Bird et al.'s study (2006), present stress directions in Southern Africa were obtained through overcoring (a type of in situ stress measurement in which small strains are produced after the stress release around a cylinder at the end of a borehole), from seismic focal mechanisms and from field observations of faults which likely formed during the Holocene Epoch. Unfortunately, all three of these sources are subject to a bit of bias. Nonetheless, the information obtained was used to create a general sense of stress and strain directions and regimes in the area. Stress regimes were predicted by looking at the orientation of the principle stress axes: normal and reverse faulting (NF) occurs when the most compressive stress axis (σ_1) is vertical; strike-slip faulting (SS) occurs where σ_2 is vertical and thrust faulting (TF) occurs when σ_3 is vertical (see Anderson's Theory in the previous section). To accommodate for mixed regimes, "NS" is used to denote a NF regime with a SS component and "TS" signifies a TF regime with a SS component.
According to the data compiled into the World Stress Map (WSM) there exists a vast region that extends from southwest Angola to South Africa in which the most compressive horizontal principal stress (σ_{1H}) is orientated NW to NNW, called the Wegener Stress Anomaly (WSA) (Andreoli et al., 1996; Viola et al., 2005). Initially, it was thought that the WSA is caused by ridge push (horizontal compression in old seafloor adjacent to a spreading rise) generated by the South West Indian Ridge (Viola et al., 2005). On the inland parts of Southern Africa, the primary stress field is one of horizontal tension in a NE-SW direction, branching from the offshore oceanic tension belt at the Indian Ocean margin between 15˚ - 25˚ latitude (Bird et al. in 2006). This stress field continues southwest through the Kaapvaal Craton and offshore into the east Atlantic Ocean (here this stress component becomes σ_{2H}, because there is an even stronger NW-SE tensional component).

Through investigation of the three stress sources mentioned earlier, Bird et al. (2006) reached two conclusions, one of which pertains to this study, namely: The quality of the predicted stress field increases by changing the basal drag from passive to active, which in turn increases the rate of relative rotation between the African- and Somalia Plates. Hence, it is suggested that the WSA and other features of Southern Africa's stress field are mainly due the resistance of unbroken lithosphere to relative plate rotation, with only minor contributions from other sources such as ridge push (Bird et al. 2006

Table 2: Most Compressive Horizontal Principal Stress Azimuths and Stress Regimes in Southern Africa*. After Bird et al., 2006

Latitude (deg.)	Longitude (deg.)	σ_{1H} Azimuth	Type	Quality	Regime	Deth (Km)	Location	Source
-34.783	19.633	115	GFS	A	NF	0	Gansbaai-Quoin Point, South Africa	Andreoli et al. [1996]
-35.170	22.150	145	BO	B	NF	0	Bredasdorp Basin, offshore South Africa	Andreoli et al. [1996]
-30.200	18.400	148	GF	A	NF	0	Santab se Vloer normal faults, Bushmanland	Brandt et al. [2005]
-24.700	16.000	172	GF	A	NS	0	Hebron dextral-normal fault, Namibia	Viola et al. [2005]
-19.900	21.900	40	GF	A	NF	0	Gumare fault, Okawango Delta, Botswana	McCarthy et al. [2002]
-19.640	23.600	39	GF	A	NF	0	Kunyere Fault, Okawango Delta, Botswana	McCarthy et al. [2002]
-19.680	23.800	42	GF	A	NF	0	Thamalakane Fault, Okawango Delta, Botswana	McCarthy et al. [2002]
-17.417	14.250	173	OC	A	TF	0.134	Ruacana Power Sta. RSM 7 and 8, Namibia	Stacey and Wesseloo [1998]
-24.000	34.500	0	GF	B	NF	0	Funhalouro-Mazenga Graben, Mozambique	Ferro and Bouman [1987]
-30.350	15.100	145	GF	A	SS	0	Offshore sinistral(?) ‘‘mud volcano’’ fault	Viola et al. [2005]
-26.500	17.600	167	GF	A	NF	0	Dreylingen-Pfalz oblique-slip fault, Namibia	Viola et al. [2005]
-29.667	22.750	160	OC	A	SS	0.8	Prieska mine, Namaqualand	Andreoli et al. [1996]
-27.800	17.260	167	GF	B	NF	0	Skorpion mine, Namibia	Viola et al. [2005]
-25.667	27.250	135	OC	C	NF	0	Rustenburg and Northam mines, Witwatersrand	Andreoli et al. [1996]
-29.700	17.900	145	OC	A	SS	1.57	Carolusberg mine, Springbok, Namaqualand	Viola et al. [2005]
-29.300	18.800	92	OC	A	SS	0.416	Black Mountain mine, Aggeneys, Namaqualand	Viola et al. [2005]
-21.383	15.367	152	GF	B	TF	0	Otombawe-Elim-Vrede reverse faults, Namibia	Klein [1980]

*** Not already in World Stress Map. Conventions used from the World Stress Map: Azimuth is measured in degrees clockwise from north. Type includes OC overcoring, GFS geologic fault slip orientation, and BO borehole breakout orientation. Quality standards were defined by Zoback and Zoback [1989]. Abbreviations used for regimes are explained in the text.**

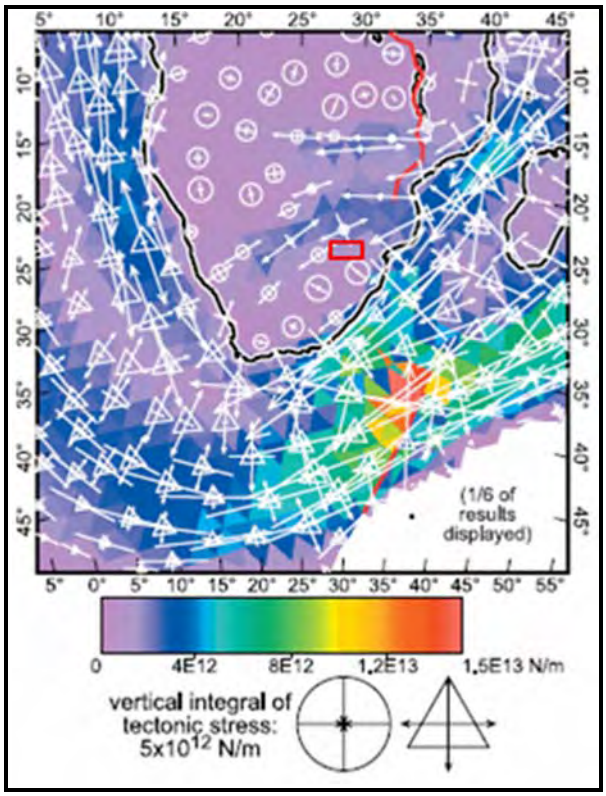

Figure 12: Vertical integrals, through the model lithosphere, of the tectonic stress tensor (symbols) and of the greatest shear stress (colours), for the preferred model AFSO- 013 by Bird et al., 2006. Circles show negative vertical components of the vertical integrals of tectonic stress (on land and in shallow water), and triangles show positive vertical components of the vertical integral of tectonic stress (in ocean basins deeper than the reference spreading ridge). Tensor symbols for vertical integrals of tectonic stress are scaled by radius (not area), and the reference symbols in the margin portray isotropic compression and tension, respectively. After Bird et al. 2006. Red rectangle indicates the study area for this thesis.

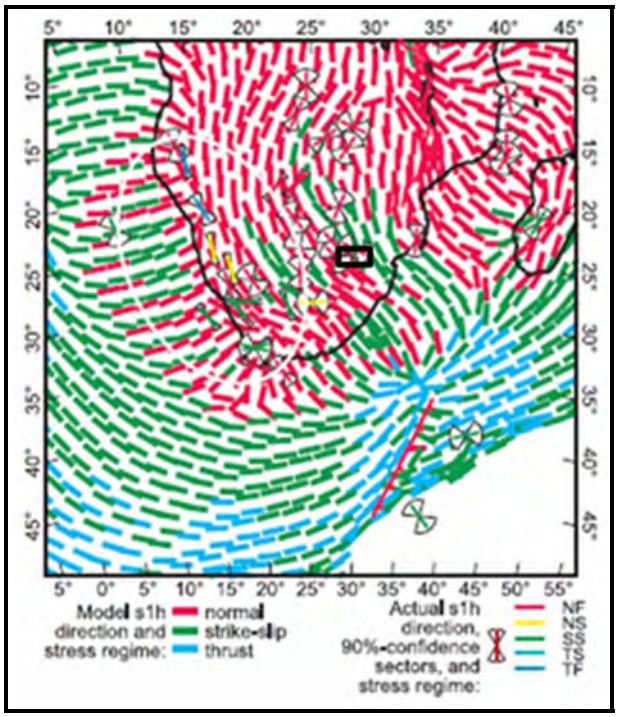

Figure 13: A map showing the most compressive horizontal principal stress directions (σ_{1H}) from AF-SO-013, the preferred model from Bird et al., 2006. Interplate indicators of stress regime are indicated in colour in the legend and the orientations of the coloured lines on the map indicate the azimuth of σ_{1H} at each location. The approximate region of the Wegener stress anomaly (Wegener stress direction province) is suggested by the white ellipse and the black rectangle indicates the study area for this thesis. After Bird et al. 2006.

Overall, the model preferred by Bird et al. (2006) (Model AF-SO-013) shows a belt of highly extensional strain rates running southward along the East African Rift. This belt branches at 12˚ south to avoid the strong region around the Kaapvaal Craton (called the Transgariep

Plate by Hartnady, 2002). The western branch connects to a western arch through Angola, Namibia and South Africa, whereas the eastern branch becomes a less active south-eastern fan which passes offshore through northern Mozambique. A prominent belt of NE-SW instrumental seismicity in South Africa is also a feature of the model predictions, where NE-SW extension is predicted to occur at about 1 x 10^{-16} s^{-1} (Bird et al. 2006). This implies that the earthquakes associated (temporally and spatially) with deep mining in South Africa may be fundamentally natural tectonic earthquakes that have been triggered or accelerated by human intervention.

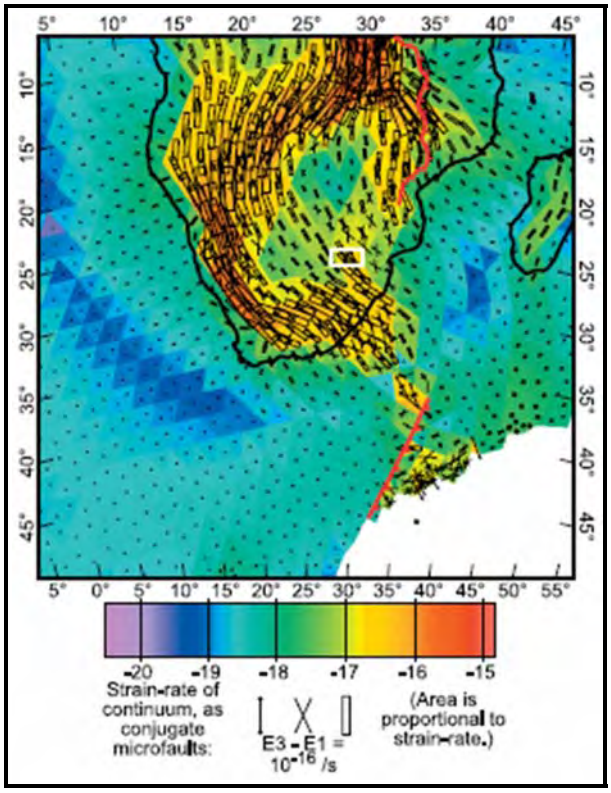

Figure 14: Long-term average (anelastic) strain rates predicted by Bird's (2006) preferred model, AF-SO-013. Color indicates the common logarithm of the magnitude of the principal strain rate with greatest absolute value (in units of s_1). Symbols show orientation of the strain rate tensor in terms of the strikes of conjugate microfaults predicted. Rectangles represent grabens; dumbbells with diamond-shaped terminations represent thrust faults and crosses indicate conjugate strike-slip faults. After Bird et al., 2006. The white rectangle indicates the study area for this thesis.

As in various other studies, artificial models cannot always sufficiently explain natural phenomena and even the preferred model created by Bird et al. (2006) has some discrepancies which have been pointed out. Firstly, in an area adjacent to this paper's focus, one finds the ENE-WSW Tshipise-Bosbokpoort Fault System, striking almost perpendicular to the computed σ_{1H}, even though the predicted regimes in the area are NF and SS. This fault system is >170km long with a well developed and preserved 2m – 10m high scarp (Brandl, 1995). Furthermore, reactivations of the Tshipise-Bosbokpoort Fault have been dated at 101 ka (estimated magnitude ~8), 101–37.5 ka (~6.6), 37.5 ka (~7.6) and 29.3 ka (~6.6) by the U-Th disequilibrium method (T. Partridge, unpublished data). Other inconsistencies regarding Bird's (2006) model includes the historical seismicity, late Pleistocene-Holocene thrust faulting (striking ENE-WSW) and soil liquefaction features in

the southern Kaapvaal Craton (Andreoli et al., 1996). Consequently, much remains to be learned about the complex faulting in certain parts of South Africa.

To sum up Bird et al.'s (2006) study one can say that although Southern Africa is surrounded by spreading ridges, most of it is not in a state of horizontal compression. On the contrary, Southern Africa is generally in a state of horizontal extension due to its high elevations which causes the density moment to be higher than those of the spreading ridges. While the NW-SE band of NW-SE directed most compressive horizontal principal stress (the Wegener stress anomaly) does exist, in many places it is actually caused by NE-SW extensional tectonics (Bird et al. in 2006). As mentioned before, this tension results from the unbroken lithosphere's resistance to relative rotation between the Somalia- and African Plates.

2.4. Previous work pertaining to structural geology's influence on groundwater in the Limpopo Belt:

A study similar to the one discussed by this report was conducted at two locations in the Central Zone (CZ) of the Limpopo Belt by Sami et al. (2002) from the Water Research Commission of South Africa. The first location falls within the Bochum- and Soutpansberg Districts and the second location forms a block between Messina, Tshipise, Gaandrik and Esmefour. Although this paper's study was conducted in the Southern Marginal Zone of the Limpopo Belt, the structural information from the adjacent Central Zone is very useful as the stress regimes causing the structures were not necessarily confined to either of these zones.

STRUCTURES IN PRE-KAROO LITHOLOGIES

First of all, Sami et al. (2002) investigated the structures in pre-Karoo lithologies. It was found that joints are best developed in more siliceous, homogenous lithologies such as granitic orthogneisses and quartz veins, as compared to poor jointing in heterogenous banded supracrustals. The ages of fractures vary from the earliest deformation recorded in the Soutpansberg Group to the young structures that formed during the breakup of Gondwana during Karoo times, as well as structures (if any) developed during post Karoo uplift (Sami et al., 2002). Joints found in pre-Karoo lithologies at location I are dominated by steep dips (>70˚) suggesting a sub-horizontal, extensional environment during formation. Strikes of these joints are predominantly orientated ~N, NW and WNW, where the latter two directions are similar to those found at location II. Most of the joints found in pre-Karoo lithologies at location II also dip steeply (>60˚), but numerous joints with dips <60˚ are also present. The joints dipping <60˚ are likely from the sinistral transpressional faulting observed by Jansen (1975) and Barker (1983). Joints found in pre-Karoo lithologies at location II strike mainly NW to N, with fewer groups striking NE and ENE (Sami et al., 2002).

STRUCTURES IN KAROO-AGED LITHOLOGIES

Karoo-aged lithologies that were investigated by Sami et al. (2002) include sandstones mudrocks and siltstones from the Clarens Formation, Karoo basalts and dolerite dykes. The best developed joints are found in the basalts and dolerites, with lesser joints in the sandstones and mudstones respectively. Karoo-aged joints found at location I once again dip steeply (>70˚) and strike in two main directions, WNW and NE. In location II, Karoo-aged joints dip >60˚, almost without exception and strike ENE to E with minor NNE orientations (Sami et al., 2002). ENE to E-striking joint and dyke orientations are consistent with the extensional regime that existed during Gondwana fragmentation. An inferior NNW direction which suggests ENE extension also exists and correlates with the two-stage Gondwana fragmentation described by Cox (1992) and Grantham (1996).

HYPOTHESIS IN TERMS OF TARGETS FOR GROUNDWATER

When exploring for groundwater, brittle structures that have been subjected to tension for a relatively long time are usually good targets. For this reason Sami et al. (2002) believe that structures striking almost perpendicular to the N-S extension since Waterberg times (such as the Bosbokpoort-Tshipise faults discussed in the previous section) are promising targets for groundwater. Furthermore, it is believed that NW and NE striking structures that have been reactivated by shear might also be good groundwater targets depending on the lithology in which such structures are found (Sami et al., 2002). This belief probably holds some truth, as Anderson and Ainslie (1994) conducted a study in the same area as location I of Sami et al. (2002) and found that NNE and NNW structures were most successful in terms of groundwater exploration.

GROUNDWATER DRILLING RESULTS

Through exploration drilling, Sami et al. (2002) discovered that regional scale normal faults are the most important water bearing targets in their study area, especially rejuvenated shear systems. Small-scale faults and local-scale structures can contain groundwater, but have lower groundwater potentials. Alluvial deposits and deeply weathered overburden (deep weathering on NW or NE striking faults) are additional aquifers. Regions where streams dog-leg in an easterly direction are especially favourable for groundwater. Interestingly, lithological contacts and dyke/sill structures were found to be dry or low yielding, but some ENE tectonic contacts were water-bearing (Sami et al., 2002).